Effective Lagrangian for $\bar{q}\tilde{q}'_i\chi^+_j$, $\bar{q}\tilde{q}_i\chi^0_j$ interactions and fermionic decays of the squarks with *CP* phases

Tarek Ibrahim* and Pran Nath

Department of Physics, Northeastern University, Boston, Massachusetts 02115-5000, USA
(Received 22 November 2004; published 18 March 2005)

We compute the one loop corrected effective Lagrangian for the quark-squark-chargino and quark-squark-neutralino interactions. The effective Lagrangian takes into account the loop corrections arising from the exchange of the gluinos, charginos, neutralinos, W, Z, the charged Higgs, and the neutral Higgs. We further analyze the squark decays into charginos and neutralinos and discuss the effect of the loop corrections on them. The analysis takes into account *CP* phases in the soft parameters. It is found that the loop corrections to the stop decay widths into chargino and neutralinos can be as much as 30% or even larger. Further, the stop decay widths show a strong dependence on the *CP* phases. These results are of relevance in the precision predictions of squark decays in the context of specific models of soft breaking in supergravity and string based models.

DOI: 10.1103/PhysRevD.71.055007 PACS numbers: 14.80.Ly, 12.60.Jv

I. INTRODUCTION

The $\bar{q}\tilde{q}'_i\chi^+_j$ and $\bar{q}\tilde{q}_i\chi^0_j$ interactions are of great interest since they enter in the decay of squarks. We expect that such decays will be observed at the collider experiments. Specifically one expects under the usual naturalness criteria that most of the [sparticles] should become visible at the Large Hadron Collider (LHC) with the possibility that some of the sparticles may also become visible at RUN II of the Tevatron. Specifically, some of the sparticles will be sfermions, i.e., squarks and sleptons, whose decay patterns include fermionic or bosonic final states [1,2]. Measurements of sparticle masses and of their decay branching ratios will be a primary focus of attention after the discovery of such particles, while a more precise measurement will come eventually at the next linear collider. With the above in mind, it is of great importance to refine the theoretical computations of the decay branching ratios beyond the tree level predictions [2] taking into account the loop corrections. In previous works, only partial analyses have been given where some of the loop diagrams have been computed analytically [3–5] while others are computed only numerically [6] or omitted altogether.

In this paper, we give the first complete analysis of all the allowed one loop diagrams analytically in a consistent manner within the framework of a zero external momentum approximation. For this purpose, it is found advantageous to compute the one loop corrected effective Lagrangian for the $\bar{q}\tilde{q}'_i\chi^+_j$ and $\bar{q}\tilde{q}_i\chi^0_j$ couplings. In the analysis we also include in addition the effect of *CP* phases. It is now well known that large *CP* phases can be made compatible [7–10] with the experimental constraints on the electric dipole moments (edms) of the electron [11], of the neutron [12], and of the Hg^{199} atom [13]. Further, if the phases are large they could affect a whole host of low energy phenomena. These include the effect on the Higgs masses, couplings and decays [14–19], dark matter [20,21], and a variety of other phenomena [22]. The outline of the rest of the paper is as follows: In Sec. II we compute the effective Lagrangian for the $\bar{t}\tilde{b}_i\chi^+_j$ and $\bar{b}\tilde{t}_i\chi^C_j$ interactions. In Sec. III a similar analysis is done for the $\bar{q}\tilde{q}_i\chi^0_j$ interaction. In Sec. IV we give an analysis of the decay widths of the squarks into charginos and neutralinos using the effective Lagrangian. In Sec. V we give a numerical analysis of the size of the loop effects on the decay widths. We also study in this section the effect of *CP* phases on the decay widths. Conclusions are given in Sec. VI.

II. EFFECTIVE LAGRANGIAN FOR $\bar{q}\tilde{q}'_i\chi^\pm_j$ INTERACTION

In this section we study the effect of loop corrections on $\bar{t}\tilde{b}_i\chi^+_j$ and on $\bar{b}\tilde{t}_i\chi^c_j$ interactions. We begin with the tree level Lagrangian density

$$\mathcal{L} = g\bar{t}(R_{bij}P_R + L_{bij}P_L)\tilde{\chi}^+_j\tilde{b}_i + g\bar{b}(R_{tij}P_R + L_{tij}P_L)\tilde{\chi}^c_j\tilde{t}_i + \text{H.c.} \quad (1)$$

where

$$R_{bij} = -(U_{j1}D_{b1i} - K_bU_{j2}D_{b2i})L_{bij} = K_tV^*_{j2}D_{b1i}$$
$$R_{tij} = -(V_{j1}D_{t1i} - K_tV_{j2}D_{t2i})L_{tij} = K_bU^*_{j2}D_{t1i} \quad (2)$$

and where

$$K_{t(b)} = \frac{m_{t(b)}}{\sqrt{2}m_W\sin\beta(\cos\beta)} \quad (3)$$

and the matrices U, V and $D_{b(t)}$ are the diagonalizing matrices of the chargino and squark mass matrices so that

*Permanent address: Department of Physics, Faculty of Science, University of Alexandria, Alexandria, Egypt.

$$U^* M_{\chi^+} V^{-1} = \mathrm{diag}(m_{\chi_1^+}, m_{\chi_2^+})$$
$$D_q^\dagger M_{\tilde{q}}^2 D_q = \mathrm{diag}(m_{\tilde{q}_1}^2, m_{\tilde{q}_2}^2) \quad (4)$$

where $m_{\chi_i^+}$ $(i = 1, 2)$ are the eigenvalues of the chargino mass matrix and $m_{\tilde{q}_I}^2$ $(i = 1, 2)$ are the eigenvalues of the squark mass^2 matrix. The loop corrections produce shift in the couplings of Eq. (2) as follows:

$$\mathcal{L}_{\rm eff} = g\bar{t}[(R_{bij} + \Delta R_{bij})P_R + (L_{bij} + \Delta L_{bij})P_L]\tilde{\chi}_j^+ \tilde{b}_i + g\bar{b}[(R_{tij} + \Delta R_{tij})P_R + (L_{tij} + \Delta L_{tij})P_L]\tilde{\chi}_j^c \tilde{t}_i + \text{H.c.} \quad (5)$$

where ΔR_{bij}, ΔL_{bij}, ΔR_{tij}, and ΔL_{tij} are the corrections that arise from the diagrams in Figs. 1–4. As is conventional we will use the zero external momentum approximation in the analysis of these corrections (see, e.g., Ref. [23]). A more complete analysis would require taking into account a finite external momentum which, however, is outside the scope of this work.

A. ΔR_{bij} and ΔL_{bij} analysis

Contributions to ΔR_{bij} and ΔL_{bij} arise from the nine loop diagrams of Fig. 1. We discuss now in detail the contribution of each of these diagrams, Figs. 1(a)–1(i). We begin with the loop diagram of Fig. 1(a) which contributes the following to ΔR_{bij} and ΔL_{bij}:

$$\Delta R_{bij}^{(1)} = \frac{2\alpha_s}{3\pi} \sum_{k=1}^{2} K_b U_{j2} D_{t1k}^* D_{b1i} e^{i\xi_3} D_{t1k} m_b m_{\tilde{g}} f(m_{\tilde{b}}^2, m_{\tilde{g}}^2, m_{\tilde{t}_k}^2) \quad (6)$$

$$\Delta L_{bij}^{(1)} = -\frac{2\alpha_s}{3\pi} \sum_{k=1}^{2} (V_{j1}^* D_{t1k}^* - K_t V_{j2}^* D_{t2k}^*) D_{t2k} D_{b2i} e^{-i\xi_3} m_b m_{\tilde{g}} f(m_{\tilde{b}}^2, m_{\tilde{g}}^2, m_{\tilde{t}_k}^2) \quad (7)$$

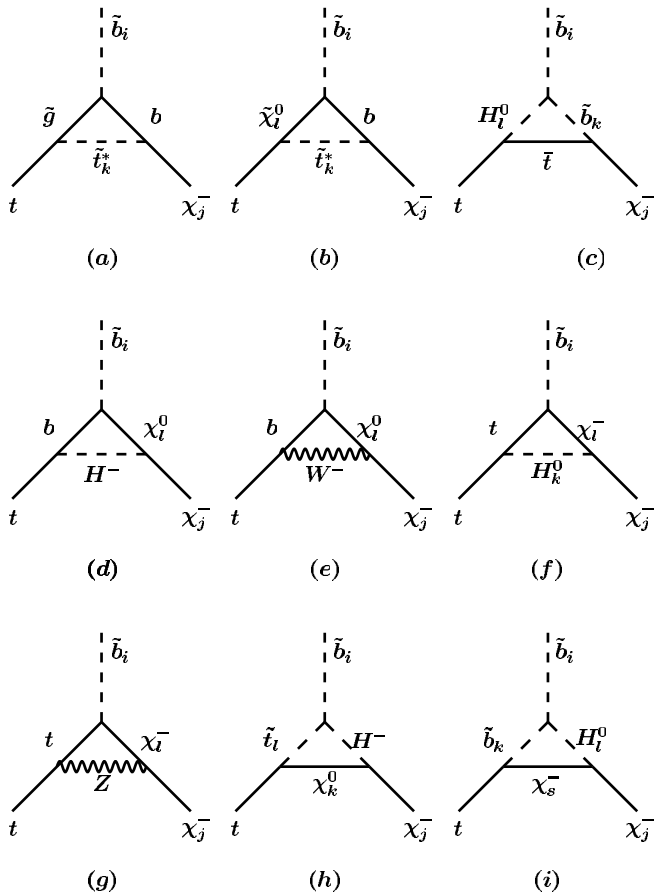

FIG. 1. List of one loop graphs that contribute to the $\bar{\tilde{b}}_i t \chi_j^-$ couplings arising from the exchange of the gluino, charginos, neutralinos, W, Z, charged Higgs and neutral Higgs.

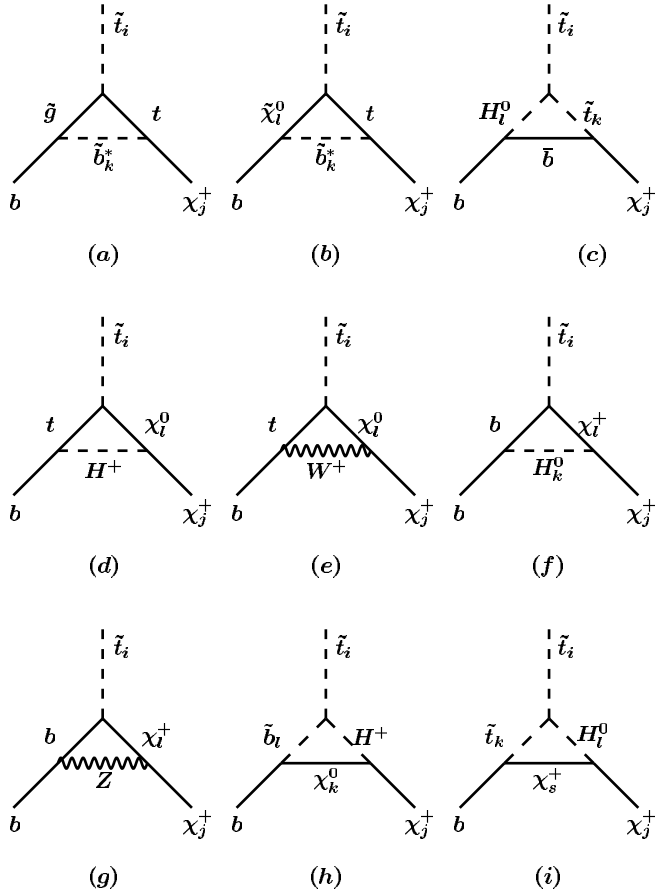

FIG. 2. List of one loop graphs that contribute to the $\bar{\tilde{t}}_i b \chi_j^+$ couplings arising from the exchange of the gluino, charginos, neutralinos, W, Z, charged Higgs and neutral Higgs.

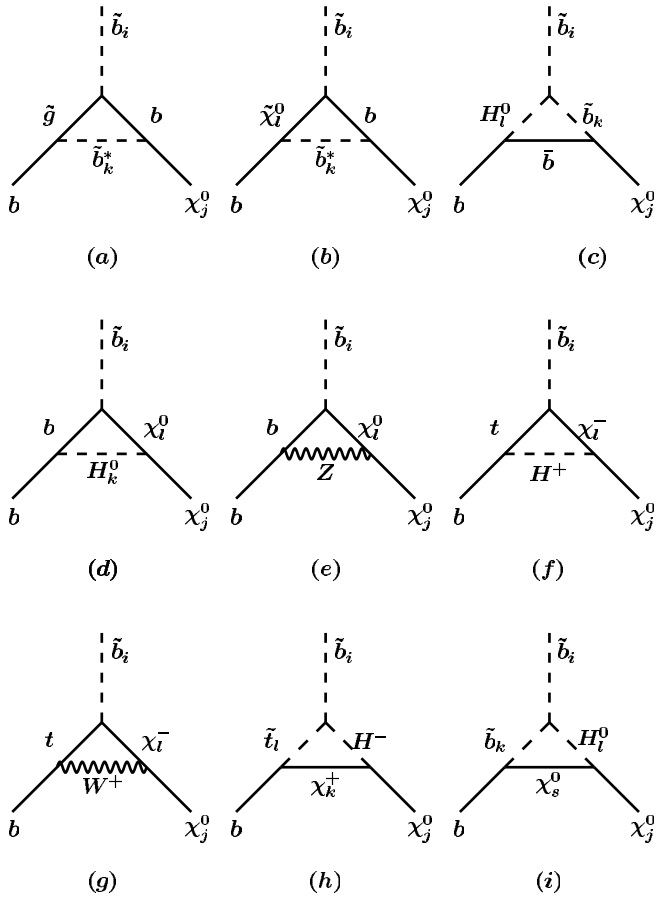

FIG. 3. List of one loop graphs that contribute to the $\bar{\tilde{b}}_i b\chi_j^+$ couplings arising from the exchange of the gluino, charginos, neutralinos, W, Z, charged Higgs and neutral Higgs.

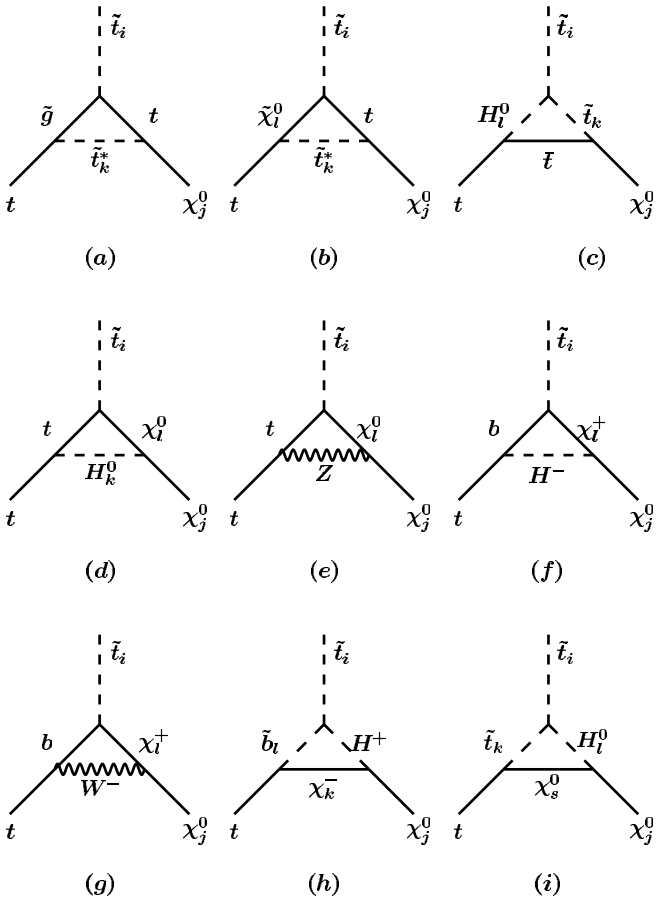

FIG. 4. List of one loop graphs that contribute to the $\bar{\tilde{t}}_i t\chi_j^+$ couplings arising from the exchange of the gluino, charginos, neutralinos, W, Z, charged Higgs and neutral Higgs.

where

$$f(x,y,z) = \frac{1}{(x-y)(x-z)(z-y)} \times \left(zx\ln\frac{z}{x} + xy\ln\frac{x}{y} + yz\ln\frac{y}{z} \right). \quad (8)$$

Next for the loop Fig. 1(b) we find

$$\Delta R_{bij}^{(2)} = \sum_{k=1}^{2}\sum_{l=1}^{4} 2K_b U_{j2} D_{t1k}^* (\beta_{bl} D_{b1i} + \alpha_{bl}^* D_{b2i}) \times (\beta_{tl} D_{t1k} + \alpha_{tl}^* D_{t2k}) \frac{m_b m_{\chi_l^0}}{16\pi^2} f(m_b^2, m_{\chi_l^0}^2, m_{\tilde{t}_k}^2) \quad (9)$$

$$\Delta L_{bij}^{(2)} = -\sum_{k=1}^{2}\sum_{l=1}^{4} 2(V_{j1}^* D_{t1k}^* - K_t V_{j2}^* D_{t2k}^*) \times (\alpha_{bl} D_{b1i} - \gamma_{bl} D_{b2i})(\alpha_{tl} D_{t1k} - \gamma_{tl} D_{t2k}) \times \frac{m_b m_{\chi_l^0}}{16\pi^2} f(m_b^2, m_{\chi_l^0}^2, m_{\tilde{t}_k}^2) \quad (10)$$

$$\begin{aligned} \alpha_{b(t)k} &= \frac{g m_{b(t)} X_{3(4)k}}{2 m_W \cos\beta(\sin\beta)} \\ \beta_{b(t)k} &= e Q_{b(t)} X_{1k}'^* + \frac{g}{\cos\theta_W} X_{2k}'^* (T_{3b(t)} - Q_{b(t)} \sin^2\theta_W) \gamma_{b(t)k} \\ &= e Q_{b(t)} X_{1k}' - \frac{g Q_{b(t)} \sin^2\theta_W}{\cos\theta_W} X_{2k}' \end{aligned} \quad (11)$$

where X''s are given by

$$\begin{aligned} X_{1k}' &= X_{1k}\cos\theta_W + X_{2k}\sin\theta_W \\ X_{2k}' &= -X_{1k}\sin\theta_W + X_{2k}\cos\theta_W \end{aligned} \quad (12)$$

and where X is the matrix that diagonalizes the neutralino mass matrix so that

$$X^T M_{\chi^0} X = \mathrm{diag}(m_{\chi_1^0}, m_{\chi_2^0}, m_{\chi_3^0}, m_{\chi_4^0}). \quad (13)$$

Figure 1(c) contributes the following:

$$\Delta R^{(3)}_{bij} = \frac{1}{\sqrt{2}} \sum_{k=1}^{2}\sum_{l=1}^{3}(U_{j1}D_{b1k} - k_b U_{j2}D_{b2k}) \times [G_{ki}(Y_{l2} + iY_{l3}\cos\beta) + G^*_{ik}(Y_{l2} - iY_{l3}\cos\beta) + H_{ki}(Y_{l1} + iY_{l3}\sin\beta) + H^*_{ik}(Y_{l1} - iY_{l3}\sin\beta)](C^S_{tl} + iC^P_{tl}) \times \frac{m_t}{16\pi^2} f(m_t^2, m^2_{\tilde{b}_k}, m^2_{H_l}) \quad (14)$$

where Y is the diagonalizing matrix of the Higgs mass^2 matrix

$$YM^2_{\rm Higgs}Y^T = {\rm diag}(m^2_{H_1}, m^2_{H_2}, m^2_{H_3}) \quad (15)$$

and

$$G_{ij} = \frac{gm_Z}{\sqrt{2}\cos\theta_W}\left[\left(-\frac{1}{2} + \frac{1}{3}\sin^2\theta_W\right)D^*_{b1i}D_{b1j} - \frac{1}{3}\sin^2\theta_W D^*_{b2i}D_{b2j}\right]\sin\beta + \frac{gm_b}{\sqrt{2}m_W\cos\beta}\mu D^*_{b1i}D_{b2j} \quad (16)$$

$$H_{ij} = -\frac{gm_Z}{\sqrt{2}\cos\theta_W}\left[\left(-\frac{1}{2} + \frac{1}{3}\sin^2\theta_W\right)D^*_{b1i}D_{b1j} - \frac{1}{3}\sin^2\theta_W D^*_{b2i}D_{b2j}\right]\cos\beta - \frac{gm_b^2}{\sqrt{2}m_W\cos\beta} \times [D^*_{b1i}D_{b1j} + D^*_{b2i}D_{b2j}] - \frac{gm_b m_0 A_b}{\sqrt{2}m_W\cos\beta}D^*_{b2i}D_{b1j} \quad (17)$$

and

$$\begin{aligned} C^S_{tl} &= \tilde{C}^S_{tl}\cos\chi_t - \tilde{C}^P_{tl}\sin\chi_t \\ C^P_{tl} &= \tilde{C}^S_{tl}\sin\chi_t + \tilde{C}^P_{tl}\cos\chi_t \\ \sqrt{2}\tilde{C}^S_{tl} &= {\rm Re}(h_t + \delta h_t)Y_{l2} + [-{\rm Im}(h_t + \delta h_t)\cos\beta + {\rm Im}(\Delta h_t)\sin\beta] \times Y_{l3} + {\rm Re}(\Delta h_t)Y_{l1} \\ \sqrt{2}\tilde{C}^P_{tl} &= -{\rm Im}(h_t + \delta h_t)Y_{l2} + [-{\rm Re}(h_t + \delta h_t)\cos\beta + {\rm Re}(\Delta h_t)\sin\beta] \times Y_{l3} - {\rm Im}(\Delta h_t)Y_{l1} \end{aligned} \quad (18)$$

with

$$\tan\chi_t = \frac{{\rm Im}(\frac{\delta h_t}{h_t} + \frac{\Delta h_t}{h_t}\cot\beta)}{1 + {\rm Re}(\frac{\delta h_t}{h_t} + \frac{\Delta h_t}{h_t}\cot\beta)} \quad (19)$$

and

$$h_t = \frac{gm_t}{\sqrt{2}m_W\sin\beta}. \quad (20)$$

The corrections Δh_t and δh_t are defined in the appendix.

$$\Delta L^{(3)}_{bij} = -\frac{1}{\sqrt{2}}\sum_{k=1}^{2}\sum_{l=1}^{3}K_t V^*_{j2}D_{b1k}[G_{ki}(Y_{l2} + iY_{l3}\cos\beta) + G^*_{ik}(Y_{l2} - iY_{l3}\cos\beta) + H_{ki}(Y_{l1} + iY_{l3}\sin\beta) + H^*_{ik}(Y_{l1} - iY_{l3}\sin\beta)](C^S_{tl} - iC^P_{tl}) \times \frac{m_t}{16\pi^2} f(m_t^2, m^2_{\tilde{b}_k}, m^2_{H_l}). \quad (21)$$

Figure 1(d) gives the following contributions:

$$\Delta R^{(4)}_{bij} = \frac{\sqrt{2}}{g}\sum_{l=1}^{4}(\beta_{bl}D_{b1i} + \alpha^*_{bl}D_{b2i}) \times (B^{S*}_{bt} - B^{P*}_{bt})\xi'_{lj}\sin\beta\frac{m_b m_{\chi^0_l}}{16\pi^2}f(m_b^2, m^2_{\chi^0_l}, m^2_{H^-}) \quad (22)$$

where

$$\begin{aligned} B^S_{bt} &= -\tfrac{1}{2}(h_b + \overline{\delta h_b})e^{-i\theta_{bt}}\sin\beta + \tfrac{1}{2}\overline{\Delta h_b}e^{-i\theta_{bt}}\cos\beta - \tfrac{1}{2}(h_t + \overline{\delta h^*_t})e^{i\theta_{bt}}\cos\beta + \tfrac{1}{2}\overline{\Delta h^*_t}e^{i\theta_{bt}}\sin\beta \\ B^P_{bt} &= -(h_t + \overline{\delta h^*_t})e^{i\theta_{bt}}\cos\beta + \tfrac{1}{2}\overline{\Delta h^*_t}e^{i\theta_{bt}}\sin\beta + \tfrac{1}{2}(h_b + \overline{\delta h_b})e^{-i\theta_{bt}}\sin\beta - \tfrac{1}{2}\overline{\Delta h_b}e^{-i\theta_{bt}}\cos\beta \end{aligned} \quad (23)$$

where $\theta_{bt} = (\chi_b + \chi_t)/2$ and where χ_b is defined by the following:

$$\tan\chi_b = \frac{{\rm Im}(\frac{\delta h_b}{h_b} + \frac{\Delta h_b}{h_b}\tan\beta)}{1 + {\rm Re}(\frac{\delta h_b}{h_b} + \frac{\Delta h_b}{h_b}\tan\beta)} \quad (24)$$

and

$$h_b = \frac{gm_b}{\sqrt{2}m_W\cos\beta} \quad (25)$$

where the corrections Δh_f, δh_f, $\Delta\bar{h}_f$ and $\delta\bar{h}_f$ are defined in the appendix.

$$\Delta L^{(4)}_{bij} = \frac{\sqrt{2}}{g}\sum_{l=1}^{4}(\alpha_{bl}D_{b1i} - \gamma_{bl}D_{b2i}) \times (B^{S*}_{bt} + B^{P*}_{bt})\xi_{lj}\cos\beta\frac{m_b m_{\chi^0_l}}{16\pi^2}f(m_b^2, m^2_{\chi^0_l}, m^2_{H^-}) \quad (26)$$

where

$$\begin{aligned} \xi'_{ji} &= -gX^*_{3j}U_{i1} + \frac{g}{\sqrt{2}}X^*_{2j}U_{i2} + \frac{1}{\sqrt{2}}g\tan\theta_W X^*_{1j}U_{i2} \\ \xi_{ji} &= -gX_{4j}V^*_{i1} - \frac{g}{\sqrt{2}}X_{2j}V^*_{i2} - \frac{1}{\sqrt{2}}g\tan\theta_W X_{1j}V^*_{i2} \end{aligned} \quad (27)$$

Next we discuss the contributions from Fig. 1(e). Here on using the properties of the projection operators, i.e.,

$\gamma^\mu P_R = P_L\gamma^\mu$, $P_L P_R = 0$, and the property of Dirac γ^μ that $g_{\mu\nu}\gamma^\mu\gamma^\nu = 4$, we get

$$\Delta R^{(5)}_{bij} = 0 \tag{28}$$

and

$$\Delta L^{(5)}_{bij} = -4g\sum_{l=1}^{4} R'_{lj}(\alpha_{bl}D_{b1i} - \gamma_{bl}D_{b2i}) \times \frac{m_b m_{\chi^0_l}}{16\pi^2} f(m_b^2, m^2_{\chi^0_l}, m^2_{W^-}) \tag{29}$$

where

$$R'_{ij} = \frac{1}{\sqrt{2}}X_{3i}U_{j3} + X_{2i}U_{j1}. \tag{30}$$

Contributions from Fig. 1(f) are as follows:

$$\Delta R^{(6)}_{bij} = -g\sum_{l=1}^{2}\sum_{k=1}^{3}[Q_{jl}(Y_{k1} + iY_{k3}\sin\beta) + S_{jl}(Y_{k2} + iY_{k3}\cos\beta)](C^S_{tk} + iC^P_{tk}) \times [U_{l1}D_{b1i} - K_b U_{l2}D_{b2i}]\frac{m_t m_{\chi^-_l}}{16\pi^2} f(m_t^2, m^2_{\chi^-_l}, m^2_{H_k}) \tag{31}$$

and

$$\Delta L^{(6)}_{bij} = g\sum_{l=1}^{2}\sum_{k=1}^{3}[Q^*_{lj}(Y_{k1} - iY_{k3}\sin\beta) + S^*_{lj}(Y_{k2} - iY_{k3}\cos\beta)](C^S_{tk} - iC^P_{tk})(K_t V^*_{l2}D_{b1i}) \times \frac{m_t m_{\chi^-_l}}{16\pi^2} f(m_t^2, m^2_{\chi^-_l}, m^2_{H_k}) \tag{32}$$

where

$$Q_{ij} = \frac{1}{\sqrt{2}}U_{i2}V_{j1} \qquad S_{ij} = \frac{1}{\sqrt{2}}U_{i1}V_{j2}. \tag{33}$$

Figure 1(g) contributes as follows:

$$\Delta R^{(7)}_{bij} = \frac{4g^2}{\cos^2\theta_W}\sum_{l=1}^{2} L''_{lj}\left(\frac{2}{3}\sin^2\theta_W\right)(U_{l1}D_{b1i} - K_b U_{l2}D_{b2i}) \times \frac{m_t m_{\chi^-_l}}{16\pi^2} f(m_t^2, m^2_{\chi^-_l}, m_Z^2) \tag{34}$$

$$\Delta L^{(7)}_{bij} = \frac{4g^2}{\cos^2\theta_W}\sum_{l=1}^{2} R''_{lj}\left(\frac{1}{2} - \frac{2}{3}\sin^2\theta_W\right)K_t V^*_{l2}D_{b1i}\frac{m_t m_{\chi^-_l}}{16\pi^2} \times f(m_t^2, m^2_{\chi^-_l}, m_Z^2) \tag{35}$$

where

$$L''_{ij} = -V_{i1}V^*_{j1} - \tfrac{1}{2}V_{i2}V^*_{j2} + \delta_{ij}\sin^2\theta_W \qquad R''_{ij} = -U^*_{i1}U_{j1} - \tfrac{1}{2}U^*_{i2}U_{j2} + \delta_{ij}\sin^2\theta_W. \tag{36}$$

The contribution of Fig. 1(h) is as follows:

$$\Delta R^{(8)}_{bij} = -\frac{\sqrt{2}}{g}\sum_{l=1}^{2}\sum_{k=1}^{4}\xi'_{kj}\sin\beta(\beta_{tk}D_{t1l} + \alpha^*_{tk}D_{t2l}) \times (\eta_{il}\cos\beta + \eta'^*_{il}\sin\beta)\frac{m_{\chi^0_k}}{16\pi^2} f(m^2_{\chi^0_k}, m^2_{H^-}, m^2_{\tilde{t}_l}) \tag{37}$$

and

$$\Delta L^{(8)}_{bij} = -\frac{\sqrt{2}}{g}\sum_{l=1}^{2}\sum_{k=1}^{4}\xi_{kj}\cos\beta(\alpha_{tk}D_{t1l} - \gamma_{tk}D_{t2l}) \times (\eta_{il}\cos\beta + \eta'^*_{il}\sin\beta)\frac{m_{\chi^0_k}}{16\pi^2} f(m^2_{\chi^0_k}, m^2_{H^-}, m^2_{\tilde{t}_l}) \tag{38}$$

where

$$\eta_{ij} = \frac{gm_t}{\sqrt{2}m_W\sin\beta}m_0 A_t D_{b1i}D^*_{t2j} + \frac{gm_b}{\sqrt{2}m_W\cos\beta}\mu D_{b2i}D^*_{t1j} + \frac{gm_b m_t}{\sqrt{2}m_W\sin\beta}D_{b2i}D^*_{t2j} + \frac{gm_t^2}{\sqrt{2}m_W\sin\beta}D_{b1i}D^*_{t1j} - \frac{g}{\sqrt{2}}m_W\sin\beta D_{b1i}D^*_{t1j} \tag{39}$$

and

$$\eta'_{ji} = \frac{gm_b}{\sqrt{2}m_W\cos\beta}m_0 A_b D^*_{b2j}D_{t1i} + \frac{gm_t}{\sqrt{2}m_W\sin\beta}\mu D^*_{b1j}D_{t2i} + \frac{gm_b m_t}{\sqrt{2}m_W\cos\beta}D^*_{b2j}D_{t2i} + \frac{gm_b^2}{\sqrt{2}m_W\cos\beta}D^*_{b1j}D_{t1i} - \frac{g}{\sqrt{2}}m_W\cos\beta D^*_{b1j}D_{t1i}. \tag{40}$$

Finally the contribution from Fig. 1(i) is as follows:

$$\Delta R^{(9)}_{bij} = \frac{g}{\sqrt{2}}\sum_{l=1}^{3}\sum_{s=1}^{2}\sum_{k=1}^{2}\{Q_{js}(Y_{l1} + iY_{l3}\sin\beta) + S_{js}(Y_{l2} + iY_{l3}\cos\beta)\}(U_{s1}D_{b1k} - K_b U_{s2}D_{b2k})[G_{ki}(Y_{l2} + iY_{l3}\cos\beta) + G^*_{ik}(Y_{l2} - iY_{ls}\cos\beta) + H_{ki}(Y_{l1} + iY_{l3}\sin\beta) + H^*_{ik}(Y_{l1} - iY_{l3}\sin\beta)]\frac{m_{\chi^-_s}}{16\pi^2}f(m^2_{\tilde{b}_k}, m^2_{H_l}, m^2_{\chi^-_s}) \tag{41}$$

$$\Delta L^{(9)}_{bij} = -\frac{g}{\sqrt{2}}\sum_{l=1}^{3}\sum_{s=1}^{2}\sum_{k=1}^{2}\{Q^*_{sj}(Y_{l1} - iY_{l3}\sin\beta) + S^*_{sj}(Y_{l2} - iY_{l3}\cos\beta)\}(K_t V^*_{s2} D_{b1k})$$
$$\times [G_{ki}(Y_{l2} + iY_{l3}\cos\beta) + G^*_{ik}(Y_{l2} - iY_{l3}\cos\beta) + H_{ki}(Y_{l1} + iY_{l3}\sin\beta) + H^*_{ik}(Y_{l1} - iY_{l3}\sin\beta)]$$
$$\times \frac{m_{\chi^-_s}}{16\pi^2} f(m^2_{\tilde{b}_k}, m^2_{H_l}, m^2_{\chi^-_s}). \tag{42}$$

Summing the contribution from the nine loop diagrams of Fig. 1(a)–1(i) we find that ΔR_{bj} and ΔL_{bij} that appear in Eq. (5) are then given by

$$\Delta R_{bij} = \sum_{n=1}^{9} \Delta R^{(n)}_{bij} \tag{43}$$

$$\Delta L_{bij} = \sum_{n=1}^{9} \Delta L^{(n)}_{bij}. \tag{44}$$

We note that the loop diagram of Fig. 1(c) with the interchange $Z \leftrightarrow H^0_l$ vanishes in the zero external momentum approximation because the vertex is proportional to the external momentum, Similarly, the loop diagram of Fig. 1(h) with the interchange $W^- \leftrightarrow H^-$ vanishes and the loop diagram of Fig. 1(i) with the interchange $Z \leftrightarrow H^0_l$ vanishes in the zero external momentum approximation.

B. Analysis of corrections ΔR_{tij} and ΔL_{tij}

The corrections ΔR_{tij} and ΔL_{tij} arise from the nine diagrams of Fig. 2, i.e., the loops (a)–(i) of Fig. 2. We label the contribution from the nine diagrams by superscripts 1–9. Thus, for example, the contributions of Fig. 2(a) are $\Delta R^{(1)}_{tij}$ and $\Delta L^{(1)}_{bij}$ etc. We now list the contributions of the nine loops of Fig. 2. We have

$$\Delta R^{(1)}_{tij} = \frac{2\alpha_s}{3\pi} \times \sum_{k=1}^{2} K_t V_{j2} D^*_{b1k} D_{t1i} e^{i\xi_3} D_{b1k} m_t m_{\tilde{g}} f(m^2_t, m^2_{\tilde{g}}, m^2_{\tilde{b}_k}) \tag{45}$$

$$\Delta L^{(1)}_{tij} = -\frac{2\alpha_s}{3\pi}\sum_{k=1}^{2}(U^*_{j1} D^*_{b1k} - K_b U^*_{j2} D^*_{b2k}) \times D_{t2i} D_{b2k} e^{-i\xi_3} m_t m_{\tilde{g}} f(m^2_t, m^2_{\tilde{g}}, m^2_{\tilde{b}_k}) \tag{46}$$

$$\Delta R^{(2)}_{tij} = \sum_{k=1}^{2}\sum_{l=1}^{4} 2K_t V_{j2} D^*_{b1k}(\beta_{tl} D_{t1i} + \alpha^*_{tl} D_{t2i}) \times (\beta_{bl} D_{b1k} + \alpha^*_{bl} D_{b2k}) \frac{m_b m_{\chi^0_l}}{16\pi^2} f(m^2_b, m^2_{\chi^0_l}, m^2_{\tilde{t}_k}) \tag{47}$$

$$\Delta L^{(2)}_{tij} = -\sum_{k=1}^{2}\sum_{l=1}^{4} 2(U^*_{j1} D^*_{b1k} - K_b U^*_{j2} D^*_{b2k}) \times (\alpha_{tl} D_{t1i} - \gamma_{tl} D_{t2i})(\alpha_{bk} D_{b1k} - \gamma_{bl} D_{b2k}) \times \frac{m_b m_{\chi^0_l}}{16\pi^2} f(m^2_b, m^2_{\chi^0_l}, m^2_{\tilde{t}_k}) \tag{48}$$

$$\Delta R^{(3)}_{tij} = \frac{1}{\sqrt{2}}\sum_{k=1}^{2}\sum_{l=1}^{3}(V_{j1} D_{t1k} - K_t V_{j2} D_{t2k}) \times [E_{ki}(Y_{l2} + iY_{l3}\cos\beta) + E^*_{ik}(Y_{l2} - iY_{l3}\cos\beta) + F_{ki}(Y_{l1} + iY_{l3}\sin\beta) + F^*_{ik}(Y_{l1} - iY_{l3}\sin\beta)] \times (C^S_{bl} + iC^P_{bl}) \frac{m_b}{16\pi^2} f(m^2_t, m^2_{\tilde{t}_k}, m^2_{H_l}) \tag{49}$$

where

$$E_{ij} = \frac{g m_Z}{\sqrt{2}\cos\theta_W}\left[\left(\frac{1}{2} - \frac{2}{3}\sin^2\theta_W\right) D^*_{t1i} D_{t1j} + \frac{2}{3}\sin^2\theta_W D^*_{t2i} D_{t2j}\right]\sin\beta - \frac{g m_t^2}{\sqrt{2} m_W \sin\beta}[D^*_{t1i} D_{t1j} + D^*_{t2i} D_{t2j}] - \frac{g m_t m_0 A_t}{\sqrt{2} m_W \sin\beta} D^*_{t2i} D_{t1j} \tag{50}$$

$$F_{ij} = -\frac{g m_Z}{\sqrt{2}\cos\theta_W}\left[\left(\frac{1}{2} - \frac{2}{3}\sin^2\theta_W\right) D^*_{t1i} D_{t1j} + \frac{2}{3}\sin^2\theta_W D^*_{t2i} D_{t2j}\right]\cos\beta + \frac{g m_t \mu}{\sqrt{2} m_W \sin\beta} D^*_{t1i} D_{t2j} \tag{51}$$

and

$$C^S_{bl} = \tilde{C}^S_{bl}\cos\chi_b - \tilde{C}^P_{bl}\sin\chi_b$$
$$C^P_{bl} = \tilde{C}^S_{bl}\sin\chi_b + \tilde{C}^P_{bl}\cos\chi_b$$
$$\sqrt{2}\tilde{C}^S_{bl} = \mathrm{Re}(h_b + \delta h_b) Y_{l1} + [-\mathrm{Im}(h_b + \delta h_b)\sin\beta + \mathrm{Im}(\Delta h_b)\cos\beta] Y_{l3} + \mathrm{Re}(\Delta h_b) Y_{l2}$$
$$\sqrt{2}\tilde{C}^P_{bl} = -\mathrm{Im}(h_b + \delta h_b) Y_{l1} + [-\mathrm{Re}(h_b + \delta h_b)\sin\beta + \mathrm{Re}(\Delta h_b)\cos\beta] Y_{l3} - \mathrm{Im}(\Delta h_t) Y_{l2} \tag{52}$$

$$\Delta L_{tij}^{(3)} = -\frac{1}{\sqrt{2}}\sum_{k=1}^{2}\sum_{l=1}^{3} K_b U_{j2}^* D_{t1k}[E_{ki}(Y_{l2} + iY_{l3}\cos\beta) + E_{ik}^*(Y_{l2} - iY_{l3}\cos\beta) + F_{ki}(Y_{l1} + iY_{l3}\sin\beta) + F_{ik}^*(Y_{l1} - iY_{l3}\sin\beta)](C_{bl}^S - iC_{bl}^P) \times \frac{m_b}{16\pi^2} f(m_b^2, m_{\tilde{t}_k}^2, m_{H_l}^2) \quad (53)$$

$$\Delta R_{tij}^{(4)} = \frac{\sqrt{2}}{g}\sum_{l=1}^{4}(\beta_{tl} D_{t1i} + \alpha_{tl}^* D_{t2i}) \times (B_{bt}^S + B_{bt}^P)\xi_{lj}^* \cos\beta \frac{m_t m_{\chi_l^0}}{16\pi^2} f(m_t^2, m_{\chi_l^0}^2, m_{H^-}^2) \quad (54)$$

$$\Delta L_{tij}^{(4)} = \frac{\sqrt{2}}{g}\sum_{l=1}^{4}(\alpha_{tl} D_{t1i} - \gamma_{tl} D_{t2i}) \times (B_{bt}^S - B_{bt}^P)\xi_{lj}'^* \sin\beta \frac{m_t m_{\chi_l^0}}{16\pi^2} f(m_t^2, m_{\chi_l^0}^2, m_{H^-}^2) \quad (55)$$

$$\Delta R_{tij}^{(5)} = 0 \quad (56)$$

and

$$\Delta L_{tij}^{(5)} = -4g\sum_{l=1}^{4} R_{lj}'^* (\alpha_{tl} D_{t1i} - \gamma_{tl} D_{t2i}) \times \frac{m_t m_{\chi_l^0}}{16\pi^2} f(m_t^2, m_{\chi_l^0}^2, m_{W^-}^2) \quad (57)$$

$$\Delta R_{tij}^{(6)} = -g\sum_{l=1}^{2}\sum_{k=1}^{3}[Q_{lj}(Y_{k1} + iY_{k3}\sin\beta) + S_{lj}(Y_{k2} + iY_{k3}\cos\beta)](C_{bk}^S + iC_{bk}^P) \times [V_{l1} D_{t1i} - K_t V_{l2} D_{t2i}]\frac{m_b m_{\chi_l^-}}{16\pi^2} f(m_b^2, m_{\chi_l^-}^2, m_{H_k}^2) \quad (58)$$

and

$$\Delta L_{tij}^{(6)} = g\sum_{l=1}^{2}\sum_{k=1}^{3}[Q_{jl}^*(Y_{k1} - iY_{k3}\sin\beta) + S_{jl}^*(Y_{k2} - iY_{k3}\cos\beta)](C_{bk}^S - iC_{bk}^P)(K_b U_{l2}^* D_{t1i}) \times \frac{m_b m_{\chi_l^-}}{16\pi^2} f(m_b^2, m_{\chi_l^-}^2, m_{H_k}^2) \quad (59)$$

$$\Delta R_{tij}^{(7)} = -\frac{4g^2}{\cos^2\theta_W}\sum_{l=1}^{2} L_{jl}''\left(\frac{1}{3}\sin^2\theta_W\right)(V_{l1} D_{t1i} - K_t V_{l2} D_{t2i}) \times \frac{m_b m_{\chi_l^-}}{16\pi^2} f(m_b^2, m_{\chi_l^-}^2, m_Z^2) \quad (60)$$

$$\Delta L_{tij}^{(7)} = -\frac{4g^2}{\cos^2\theta_W}\sum_{l=1}^{2} R_{jl}''\left(\frac{1}{2} - \frac{1}{3}\sin^2\theta_W\right) \times K_b U_{l2}^* D_{t1i} \frac{m_t m_{\chi_l^-}}{16\pi^2} f(m_b^2, m_{\chi_l^-}^2, m_Z^2) \quad (61)$$

where

$$\Delta R_{tij}^{(8)} = -\frac{\sqrt{2}}{g}\sum_{l=1}^{2}\sum_{k=1}^{4}\xi_{jk}^* \cos\beta(\beta_{bk} D_{b1l} + \alpha_{bk}^* D_{b2l}) \times (\eta_{li}' \sin\beta + \eta_{li}'^* \cos\beta)\frac{m_{\chi_k^0}}{16\pi^2} f(m_{\chi_k^0}^2, m_{H^-}^2, m_{\tilde{b}_l}^2) \quad (62)$$

and

$$\Delta L_{tij}^{(8)} = -\frac{\sqrt{2}}{g}\sum_{l=1}^{2}\sum_{k=1}^{4}\xi_{jk}'^* \sin\beta(\alpha_{bk} D_{b1l} - \gamma_{bk} D_{b2l}) \times (\eta_{li}' \sin\beta + \eta_{li}^* \cos\beta)\frac{m_{\chi_k^0}}{16\pi^2} f(m_{\chi_k^0}^2, m_{H^-}^2, m_{\tilde{b}_l}^2) \quad (63)$$

$$\Delta R_{tij}^{(9)} = \frac{g}{\sqrt{2}}\sum_{l=1}^{3}\sum_{s=1}^{2}\sum_{k=1}^{2}\{Q_{sj}(Y_{l1} + iY_{l3}\sin\beta) + S_{sj}(Y_{l2} + iY_{l3}\cos\beta)\}(V_{s1} D_{t1k} - K_t V_{s2} D_{t2k}) \times [E_{ki}(Y_{l2} + iY_{l3}\cos\beta) + E_{ik}^*(Y_{l2} - iY_{l3}\cos\beta) + F_{ki}(Y_{l1} + iY_{l3}\sin\beta) + F_{ik}^*(Y_{l1} - iY_{l3}\sin\beta)] \times \frac{m_{\chi_s^-}}{16\pi^2} f(m_{\tilde{t}_k}^2, m_{H_l}^2, m_{\chi_s^-}^2) \quad (64)$$

$$\Delta L_{bij}^{(9)} = -\frac{g}{\sqrt{2}}\sum_{l=1}^{3}\sum_{s=1}^{2}\sum_{k=1}^{2}\{Q_{js}^*(Y_{l1} - iY_{l3}\sin\beta) + S_{js}^*(Y_{l2} - iY_{l3}\cos\beta)\}(K_b U_{s2}^* D_{t1k}) \times [E_{ki}(Y_{l2} + iY_{l3}\cos\beta) + E_{ik}^*(Y_{l2} - iY_{l3}\cos\beta) + F_{ki}(Y_{l1} + iY_{l3}\sin\beta) + F_{ik}^*(Y_{l1} - iY_{l3}\sin\beta)] \times \frac{m_{\chi_s^-}}{16\pi^2} f(m_{\tilde{t}_k}^2, m_{H_l}^2, m_{\chi_s^-}^2) \quad (65)$$

$$\Delta R_{tij} = \sum_{n=1}^{9}\Delta R_{tij}^{(n)} \quad (66)$$

$$\Delta L_{tij} = \sum_{n=1}^{9} \Delta L_{tij}^{(n)}. \tag{67}$$

The loops corresponding to Figs. 2(c) and 2(i) where $Z \leftrightarrow H_i^0$ vanishes for the same reason as discussed earlier in Sec. II A. Similarly, the loop corresponding to Fig. 2(h) with $W^+ \leftrightarrow H^+$ vanishes for the same reason.

III. THE EFFECTIVE LAGRANGIAN FOR $\bar{q}\tilde{q}_i\chi_j^0$ INTERACTION

We turn now to an analysis of the loop corrections to the squark-quark-neutralino interaction. We begin with the tree level $\bar{q}\tilde{q}_i\chi_j^0$ interaction which is given by

$$\begin{aligned}\mathcal{L} = {} & g\bar{b}[K_{bij}P_R + M_{bij}P_L]\chi_j^0\tilde{b}_i \\ & + g\bar{t}[K_{tij}P_R + M_{tij}P_L]\chi_j^0\tilde{t}_i + \text{H.c.}\end{aligned} \tag{68}$$

where

$$\begin{aligned} K_{bij} &= -\sqrt{2}[\beta_{bj}D_{b1i} + \alpha_{bj}^* D_{b2i}] \\ K_{tij} &= -\sqrt{2}[\beta_{tj}D_{t1i} + \alpha_{tj}^* D_{t2i}] \\ M_{bij} &= -\sqrt{2}[\alpha_{bj}D_{b1i} - \gamma_{bj}D_{b2i}] \\ M_{tij} &= -\sqrt{2}[\alpha_{tj}D_{t1i} - \gamma_{tj}D_{t2i}]. \end{aligned} \tag{69}$$

The loop corrections produce a shift in the couplings of Eq. (69) as follows:

$$\begin{aligned}\mathcal{L}_{\text{eff}} = {} & g\bar{b}[(K_{bij} + \Delta K_{bij})P_R + (M_{bij} + \Delta M_{bij})P_L]\chi_j^0\tilde{b}_i \\ & + g\bar{t}[(K_{tij} + \Delta K_{tij})P_R + (M_{tij} + \Delta M_{tij})P_L]\chi_j^0\tilde{t}_i \\ & + \text{H.c.}\end{aligned} \tag{70}$$

Thus in this part of the analysis we will calculate the quantities ΔK_{bij}, ΔK_{tij}, ΔM_{bij}, and ΔM_{tij} from the one loop corrections arising from Figs. 3 and 4 using as in the previous analysis the zero external momentum approximation.

A. Analysis of loop corrections to the $\bar{b}\tilde{b}_i\chi_j^0$ interaction

Loop corrections to the $\bar{b}\tilde{b}_i\chi_j^0$ interaction, i.e., ΔK_{bij} and ΔM_{bij}, arise from the nine diagrams of Fig. 3. We give now the individual contribution of these nine loops. The contribution from Fig. 3(a) is

$$\begin{aligned}\Delta K_{bij}^{(1)} = {} & -\frac{2\sqrt{2}\alpha_s}{3\pi g}\sum_{k=1}^{2} e^{i\xi_3}D_{b1i}D_{b1k}(\alpha_{bj}^* D_{b1k}^* - \gamma_{bj}^* D_{b2k}^*) \\ & \times m_b m_{\tilde{g}} f(m_b^2, m_{\tilde{g}}^2, m_{\tilde{b}_k}^2)\end{aligned} \tag{71}$$

$$\begin{aligned}\Delta M_{bij}^{(1)} = {} & -\frac{2\sqrt{2}\alpha_s}{3\pi g}\sum_{k=1}^{2} e^{-i\xi_3}D_{b2i}D_{b2k}(\beta_{bj}^* D_{b1k}^* + \alpha_{bj} D_{b2k}^*) \\ & \times m_b m_{\tilde{g}} f(m_b^2, m_{\tilde{g}}^2, m_{\tilde{b}_k}^2).\end{aligned} \tag{72}$$

Figure 3(b) contributes as follows:

$$\Delta K_{bij}^{(2)} = -\frac{2\sqrt{2}}{g}\sum_{l=1}^{4}\sum_{k=1}^{2}(\beta_{bl}D_{b1i} + \alpha_{bl}^* D_{b2i})(\beta_{bl}D_{b1k} + \alpha_{bl}^* D_{b2k})(\alpha_{bj}^* D_{b1k}^* - \gamma_{bj}^* D_{b2k}^*)\frac{m_b m_{\chi_l^0}}{16\pi^2} f(m_b^2, m_{\chi_l^0}^2, m_{\tilde{b}_k}^2) \tag{73}$$

$$\Delta M_{bij}^{(2)} = -\frac{2\sqrt{2}}{g}\sum_{l=1}^{4}\sum_{k=1}^{2}(\alpha_{bl}D_{b1i} - \gamma_{bl}D_{b2i})(\alpha_{bl}D_{b1k} - \gamma_{bl}D_{b2k})(\beta_{bj}^* D_{b1k}^* + \alpha_{bj} D_{b2k}^*)\frac{m_b m_{\chi_l^0}}{16\pi^2} f(m_b^2, m_{\chi_l^0}^2, m_{\tilde{b}_k}^2) \tag{74}$$

Figure 3(c) makes the following contribution:

$$\begin{aligned}\Delta K_{bij}^{(3)} = {} & \frac{1}{g}\sum_{l=1}^{3}\sum_{k=1}^{2}[G_{ki}(Y_{l2} + iY_{l3}\cos\beta) + G_{ik}^*(Y_{l2} - iY_{l3}\cos\beta) + H_{ki}(Y_{l1} + iY_{l3}\sin\beta) + H_{ik}^*(Y_{l1} - iY_{l3}\sin\beta)] \\ & \times (C_{bl}^S + iC_{bl}^P)[\beta_{bj}D_{b1k} + \alpha_{bj}^* D_{b2k}]\frac{m_b}{16\pi^2} f(m_b^2, m_{H_l}^2, m_{\tilde{b}_k}^2)\end{aligned} \tag{75}$$

$$\begin{aligned}\Delta M_{bij}^{(3)} = {} & \frac{1}{g}\sum_{l=1}^{3}\sum_{k=1}^{2}[G_{ki}(Y_{l2} + iY_{l3}\cos\beta) + G_{ik}^*(Y_{l2} - iY_{l3}\cos\beta) + H_{ki}(Y_{l1} + iY_{l3}\sin\beta) + H_{ik}^*(Y_{l1} - iY_{l3}\sin\beta)] \\ & \times (C_{bl}^S - iC_{bl}^P)[\alpha_{bj}D_{b1k} - \gamma_{bj}D_{b2k}]\frac{m_b}{16\pi^2} f(m_b^2, m_{H_l}^2, m_{\tilde{b}_k}^2).\end{aligned} \tag{76}$$

Figure 3(d) contributes as follows:

$$\Delta K^{(4)}_{bij} = -\sum_{l=1}^{4}\sum_{k=1}^{3}[Q'_{lj}(Y_{k1} + iY_{k3}\sin\beta) - S'_{lj}(Y_{k2} + iY_{k3}\cos\beta)](C^S_{bk} + iC^P_{bk})(\beta_{bl}D_{b1i} + \alpha^*_{bl}D_{b2i}) \times \frac{m_b m_{\chi^0_l}}{16\pi^2} f(m_b^2, m^2_{\chi^0_l}, m^2_{H_k}) \tag{77}$$

$$\Delta M^{(4)}_{bij} = -\sum_{l=1}^{4}\sum_{k=1}^{3}[Q'^*_{jl}(Y_{k1} - iY_{k3}\sin\beta) - S'^*_{jl}(Y_{k2} - iY_{k3}\cos\beta)](C^S_{bk} - iC^P_{bk})(\alpha_{bl}D_{b1i} - \gamma_{bl}D_{b2i}) \times \frac{m_b m_{\chi^0_l}}{16\pi^2} f(m_b^2, m^2_{\chi^0_l}, m^2_{H_k}) \tag{78}$$

where

$$Q'_{ij} = \frac{1}{\sqrt{2}}[X^*_{3i}(X^*_{2j} - \tan\theta_W X^*_{1j})] \qquad S'_{ij} = \frac{1}{\sqrt{2}}[X^*_{4j}(X^*_{2i} - \tan\theta_W X^*_{1i})]. \tag{79}$$

Figure 3(e) contributes as follows:

$$\Delta K^{(5)}_{bij} = -\frac{4\sqrt{2}g}{\cos^2\theta_W}\sum_{l=1}^{4} L'''_{jl}\left(\frac{1}{3}\sin^2\theta_W\right)(\beta_{bl}D_{b1i} + \alpha^*_{bl}D_{b2i})\frac{m_b m_{\chi^0_l}}{16\pi^2} f(m_b^2, m_Z^2, m^2_{\chi^0_l}) \tag{80}$$

$$\Delta M^{(5)}_{bij} = \frac{4\sqrt{2}g}{\cos^2\theta_W}\sum_{l=1}^{4} R'''_{jl}\left(\frac{1}{2} - \frac{1}{3}\sin^2\theta_W\right)(\alpha_{bl}D_{b1i} - \gamma_{bl}D_{b2i})\frac{m_b m_{\chi^0_l}}{16\pi^2} f(m_b^2, m_Z^2, m^2_{\chi^0_l}) \tag{81}$$

$$L'''_{ij} = -\tfrac{1}{2}X^*_{3i}X_{3j} + \tfrac{1}{2}X^*_{4i}X_{4j} \qquad R'''_{ij} = -L'''^*_{ij}. \tag{82}$$

The contribution of Fig. 3(f) is

$$\Delta K^{(6)}_{bij} = \sum_{l=1}^{2}(B^S_{bt} + B^P_{bt})(U_{l1}D_{b1i} - K_b U_{l2}D_{b2i})\xi^*_{jl}\cos\beta\frac{m_t m_{\chi^-_l}}{16\pi^2} f(m_t^2, m^2_{\chi^-_l}, m^2_{H^-}) \tag{83}$$

$$\Delta M^{(6)}_{bij} = -\sum_{l=1}^{2}(B^S_{bt} - B^P_{bt})(K_t V^*_{l2}D_{b1i})\xi'^*_{jl}\sin\beta\frac{m_t m_{\chi^-_l}}{16\pi^2} f(m_t^2, m^2_{\chi^-_l}, m^2_{H^-}). \tag{84}$$

Figure 3(g) contributes as follows:

$$\Delta K^{(7)}_{bij} = 0 \tag{85}$$

$$\Delta M^{(7)}_{bij} = \frac{4g^2}{\sqrt{2}}\sum_{l=1}^{2} R'^*_{lj}K_t V^*_{l2}D_{b1i}\frac{m_t m_{\chi^-_l}}{16\pi^2} f(m_t^2, m^2_{\chi^-_l}, m_W^2). \tag{86}$$

The contribution from Fig. 3(h) is

$$\Delta K^{(8)}_{bij} = -\sum_{k=1}^{2}\sum_{l=1}^{2}\xi'_{jk}\sin\beta(V_{k1}D_{t1l} - K_t V_{k2}D_{t2l})(\eta_{il}\cos\beta + \eta'^*_{il}\sin\beta)\frac{m_{\chi^+_l}}{16\pi^2} f(m^2_{\chi^+_k}, m^2_{\tilde{t}_l}, m^2_{H^-}) \tag{87}$$

$$\Delta M^{(8)}_{bij} = \sum_{k=1}^{2}\sum_{l=1}^{2}\xi_{jk}\cos\beta(K_b U^*_{k2}D_{t1l})(\eta_{il}\cos\beta + \eta'^*_{il}\sin\beta)\frac{m_{\chi^+_l}}{16\pi^2} f(m^2_{\chi^+_k}, m^2_{\tilde{t}_l}, m^2_{H^-}). \tag{88}$$

Finally Fig. 3(i) gives

$$\Delta K^{(9)}_{bij} = \sum_{s=1}^{4}\sum_{k=1}^{2}\sum_{l=1}^{3}[G_{ki}(Y_{l2} + iY_{l3}\cos\beta) + G^*_{ik}(Y_{l2} - iY_{l3}\cos\beta) + H_{ki}(Y_{l1} + iY_{l3}\sin\beta) + H^*_{ik}(Y_{l1} - iY_{l3}\sin\beta)] \times(\beta_{bs}D_{b1k} + \alpha^*_{bs}D_{b2k})[Q'_{sj}(Y_{l1} + iY_{l3}\sin\beta) - S'_{sj}(Y_{l2} + iY_{l3}\cos\beta)]\frac{m_{\chi^0_s}}{16\pi^2} f(m^2_{\chi^0_s}, m^2_{\tilde{b}_k}, m^2_{H_l}) \tag{89}$$

$$\Delta M^{(9)}_{bij} = \sum_{s=1}^{4}\sum_{k=1}^{2}\sum_{l=1}^{3}[G_{ki}(Y_{l2} + iY_{l3}\cos\beta) + G^*_{ik}(Y_{l2} - iY_{l3}\cos\beta) + H_{ki}(Y_{l1} + iY_{l3}\sin\beta) + H^*_{ik}(Y_{l1} - iY_{l3}\sin\beta)]$$
$$\times(\alpha_{bs}D_{b1k} - \gamma_{bs}D_{b2k})[Q'^*_{js}(Y_{l1} - iY_{l3}\sin\beta) - S'^*_{js}(Y_{l2} - iY_{l3}\cos\beta)]\frac{m_{\chi^0_s}}{16\pi^2}f(m^2_{\chi^0_s}, m^2_{\tilde b_k}, m^2_{H_l}). \quad (90)$$

The sum of the contribution of the nine diagrams of Fig. 3 gives ΔK_{bij} and ΔM_{bij}

$$\Delta K_{bij} = \sum_{n=1}^{9}\Delta K^{(n)}_{bij} \qquad \Delta M_{bij} = \sum_{n=1}^{9}\Delta M^{(n)}_{bij}. \quad (91)$$

We note that the diagram corresponding to Figs. 3(c) and 3(i) with $Z \leftrightarrow H^0_l$, and the diagram corresponding to Fig. 3(h) with $W^- \leftrightarrow H^-$ vanish in the zero external momentum approximation.

B. Loop corrections to the $\bar t\tilde t_i\chi^0_j$ interaction

Loop corrections to the $\bar t\tilde t_i\chi^0_j$ interaction, i.e., ΔK_{tij} and ΔM_{tij}, arise from the nine loops of Fig. 4. We now give the explicit computation of each loop. Figure 4(a) gives

$$\Delta K^{(1)}_{tij} = -\frac{2\sqrt2\alpha_s}{3\pi g}\sum_{k=1}^{2}e^{i\xi_3}D_{t1i}D_{t1k}(\alpha^*_{tj}D^*_{t1k} - \gamma^*_{tj}D^*_{t2k})m_t m_{\tilde g}f(m^2_t, m^2_{\tilde g}, m^2_{\tilde t_k}) \quad (92)$$

$$\Delta M^{(1)}_{tij} = -\frac{2\sqrt2\alpha_s}{3\pi g}\sum_{k=1}^{2}e^{-i\xi_3}D_{t2i}D_{t2k}(\beta^*_{tj}D^*_{t1k} + \alpha_{tj}D^*_{t2k})m_t m_{\tilde g}f(m^2_t, m^2_{\tilde g}, m^2_{\tilde t_k}). \quad (93)$$

Figure 4(b) gives

$$\Delta K^{(2)}_{tij} = -\frac{2\sqrt2}{g}\sum_{l=1}^{4}\sum_{k=1}^{2}(\beta_{tl}D_{t1i} + \alpha^*_{tl}D_{t2i})(\beta_{tl}D_{t1k} + \alpha^*_{tl}D_{t2k})(\alpha^*_{tj}D^*_{t1k} - \gamma^*_{tj}D^*_{t2k})\frac{m_t m_{\chi^0_l}}{16\pi^2}f(m^2_t, m^2_{\chi^0_l}, m^2_{\tilde t_k}) \quad (94)$$

$$\Delta M^{(2)}_{tij} = -\frac{2\sqrt2}{g}\sum_{l=1}^{4}\sum_{k=1}^{2}(\alpha_{tl}D_{t1i} - \gamma_{tl}D_{t2i})(\alpha_{tl}D_{t1k} - \gamma_{tl}D_{t2k})(\beta^*_{tj}D^*_{t1k} + \alpha_{tj}D^*_{t2k})\frac{m_t m_{\chi^0_l}}{16\pi^2}f(m^2_t, m^2_{\chi^0_l}, m^2_{\tilde t_k}). \quad (95)$$

Figure 4(c) makes the following contribution:

$$\Delta K^{(3)}_{tij} = \frac{1}{g}\sum_{l=1}^{3}\sum_{k=1}^{2}[E_{ki}(Y_{l2} + iY_{l3}\cos\beta) + E^*_{ik}(Y_{l2} - iY_{l3}\cos\beta) + F_{ki}(Y_{l1} + iY_{l3}\sin\beta) + F^*_{ik}(Y_{l1} - iY_{l3}\sin\beta)]$$
$$\times(C^S_{tl} + iC^P_{tl})[\beta_{tj}D_{t1k} + \alpha^*_{tj}D_{t2k}]\frac{m_t}{16\pi^2}f(m^2_t, m^2_{H_l}, m^2_{\tilde t_k}) \quad (96)$$

$$\Delta M^{(3)}_{tij} = \frac{1}{g}\sum_{l=1}^{3}\sum_{k=1}^{2}[E_{ki}(Y_{l2} + iY_{l3}\cos\beta) + E^*_{ik}(Y_{l2} - iY_{l3}\cos\beta) + F_{ki}(Y_{l1} + iY_{l3}\sin\beta) + F^*_{ik}(Y_{l1} - iY_{l3}\sin\beta)]$$
$$\times(C^S_{tl} - iC^P_{tl})[\alpha_{tj}D_{t1k} - \gamma_{tj}D_{t2k}]\frac{m_t}{16\pi^2}f(m^2_t, m^2_{H_l}, m^2_{\tilde t_k}). \quad (97)$$

Figure 4(d) gives

$$\Delta K^{(4)}_{tij} = -\sum_{l=1}^{4}\sum_{k=1}^{3}[Q'_{lj}(Y_{k1} + iY_{k3}\sin\beta) - S'_{lj}(Y_{k2} + iY_{k3}\cos\beta)](C^S_{tk} + iC^P_{tk})(\beta_{tl}D_{t1i} + \alpha^*_{tl}D_{t2i})\frac{m_t m_{\chi^0_l}}{16\pi^2}f(m^2_t, m^2_{\chi^0_l}, m^2_{H_k}) \quad (98)$$

$$\Delta M^{(4)}_{tij} = -\sum_{l=1}^{4}\sum_{k=1}^{3}[Q'^*_{jl}(Y_{k1} - iY_{k3}\sin\beta) - S'^*_{jl}(Y_{k2} - iY_{k3}\cos\beta)](C^S_{tk} - iC^P_{tk})(\alpha_{tl}D_{t1i} - \gamma_{tl}D_{t2i})\frac{m_t m_{\chi^0_l}}{16\pi^2}f(m^2_t, m^2_{\chi^0_l}, m^2_{H_k}). \quad (99)$$

Figure 4(e) gives

$$\Delta K^{(5)}_{tij} = \frac{4\sqrt{2}g}{\cos^2\theta_W}\sum_{l=1}^{4} L'''_{jl}\left(\frac{2}{3}\sin^2\theta_W\right)(\beta_{tl}D_{t1i} + \alpha^*_{tl}D_{t2i})\frac{m_t m_{\chi^0_l}}{16\pi^2} f(m_t^2, m_Z^2, m^2_{\chi^0_l}) \tag{100}$$

$$\Delta M^{(5)}_{tij} = \frac{-4\sqrt{2}g}{\cos^2\theta_W}\sum_{l=1}^{4} R'''_{jl}\left(\frac{1}{2} - \frac{2}{3}\sin^2\theta_W\right)(\alpha_{tl}D_{t1i} - \gamma_{tl}D_{t2i})\frac{m_t m_{\chi^0_l}}{16\pi^2} f(m_t^2, m_Z^2, m^2_{\chi^0_l}). \tag{101}$$

Figure 4(f) gives

$$\Delta K^{(6)}_{tij} = \sum_{l=1}^{2}(B^{S*}_{bt} - B^{P*}_{bt})(V_{l1}D_{t1i} - K_t V_{l2}D_{t2i})\xi'_{jl}\sin\beta\frac{m_b m_{\chi^+_l}}{16\pi^2} f(m_b^2, m^2_{\chi^+_l}, m^2_{H^+}) \tag{102}$$

$$\Delta M^{(6)}_{tij} = -\sum_{l=1}^{2}(B^{S*}_{bt} + B^{P*}_{bt})(K_b U^*_{l2}D_{t1i})\xi_{jl}\cos\beta\frac{m_b m_{\chi^+_l}}{16\pi^2} f(m_b^2, m^2_{\chi^+_l}, m^2_{H^+}). \tag{103}$$

Figure 4(g) gives

$$\Delta K^{(7)}_{tij} = 0 \tag{104}$$

$$\Delta M^{(7)}_{tij} = \frac{4g^2}{\sqrt{2}}\sum_{l=1}^{2} R'_{jl}K_b U^*_{l2}D_{t1i}\frac{m_b m_{\chi^+_l}}{16\pi^2} f(m_b^2, m^2_{\chi^+_l}, m_W^2). \tag{105}$$

Figure 4(h) makes the following contribution:

$$\Delta K^{(8)}_{tij} = -\sum_{k=1}^{2}\sum_{l=1}^{2}\xi^*_{jk}\cos\beta(U_{k1}D_{b1l} - K_b U_{k2}D_{b2l})(\eta'_{li}\sin\beta + \eta^*_{li}\cos\beta)\frac{m_{\chi^-_l}}{16\pi^2} f(m^2_{\chi^-_k}, m^2_{\tilde{b}_l}, m^2_{H^+}) \tag{106}$$

$$\Delta M^{(8)}_{tij} = \sum_{k=1}^{2}\sum_{l=1}^{2}\xi'^*_{jk}\sin\beta(K_t V^*_{k2}D_{b1l})(\eta'_{li}\sin\beta + \eta^*_{li}\cos\beta)\frac{m_{\chi^-_l}}{16\pi^2} f(m^2_{\chi^-_k}, m^2_{\tilde{b}_l}, m^2_{H^+}). \tag{107}$$

Finally Fig. 4(i) gives

$$\begin{aligned}\Delta K^{(9)}_{tij} = &\sum_{s=1}^{4}\sum_{k=1}^{2}\sum_{l=1}^{3}[E_{ki}(Y_{l2} + iY_{l3}\cos\beta) + E^*_{ik}(Y_{l2} - iY_{l3}\cos\beta) + F_{ki}(Y_{l1} + iY_{l3}\sin\beta) + F^*_{ik}(Y_{l1} - iY_{l3}\sin\beta)]\\ &\times(\beta_{ts}D_{t1k} + \alpha^*_{ts}D_{t2k})[Q'_{sj}(Y_{l1} + iY_{l3}\sin\beta) - S'_{sj}(Y_{l2} + iY_{l3}\cos\beta)]\frac{m_{\chi^0_s}}{16\pi^2} f(m^2_{\chi^0_s}, m^2_{\tilde{t}_k}, m^2_{H_l})\end{aligned} \tag{108}$$

$$\begin{aligned}\Delta M^{(9)}_{tij} = &\sum_{s=1}^{4}\sum_{k=1}^{2}\sum_{l=1}^{3}[E_{ki}(Y_{l2} + iY_{l3}\cos\beta) + E^*_{ik}(Y_{l2} - iY_{l3}\cos\beta) + F_{ki}(Y_{l1} + iY_{l3}\sin\beta) + F^*_{ik}(Y_{l1} - iY_{l3}\sin\beta)]\\ &\times(\alpha_{ts}D_{t1k} - \gamma_{ts}D_{t2k})[Q'^*_{js}(Y_{l1} - iY_{l3}\sin\beta) - S'^*_{js}(Y_{l2} - iY_{l3}\cos\beta)]\frac{m_{\chi^0_s}}{16\pi^2} f(m^2_{\chi^0_s}, m^2_{\tilde{t}_k}, m^2_{H_l}).\end{aligned} \tag{109}$$

The sum of contributions above give ΔK_{bij} and ΔM_{bij} so that

$$\Delta K_{tij} = \sum_{n=1}^{9}\Delta K^{(n)}_{tij} \qquad \Delta M_{tij} = \sum_{n=1}^{9}\Delta M^{(n)}_{tij}. \tag{110}$$

As in the previous analysis, the contribution from Fig. 4(c) with the interchange $Z \leftrightarrow H^0_l$ vanishes in the zero external momentum approximation since the vertex is proportional to the external momentum. Similarly, the contribution from Fig. 4(h) with the interchange $W^- \leftrightarrow H^-$ vanishes and Fig. 4(i) with the interchange $Z \leftrightarrow H^0_l$ vanishes in the zero external momentum approximation for the same reason. We also note that loops where one of the internal lines is a gluon line also vanishes in the zero external momentum approximation since the squark-gluon interaction gives a vertex of $-ig_s(p + p')^\mu$ which is of course dependent on the momenta.

IV. LOOP CORRECTED SQUARK DECAYS INTO CHARGINOS AND NEUTRALINOS

Equations (5) and (70) give the loop corrected effective Lagrangian for $\bar{q}\tilde{q}'_i\chi^\pm_j$ and $\bar{q}\tilde{q}_i\chi^0_j$ interactions. Next we use this loop corrected Lagrangian to compute the decay widths of the third generation squarks into charginos and neutralinos. Specifically, we will analyze the following decays:

$$\begin{aligned}&\tilde{b}_i \to t + \chi^-_j \qquad \tilde{t}_i \to b + \chi^+_j \qquad \tilde{b}_i \to b + \chi^0_j\\ &\qquad\qquad \tilde{t}_i \to t + \chi^0_j.\end{aligned} \tag{111}$$

To make the analysis more compact we begin by writing

both Eqs. (5) and (70) in the following form:

$$\mathcal{L} = \bar{f}(B^S_{ij} + B^P_{ij}\gamma_S) f_j \tilde{q}_i + \text{H.c.} \tag{112}$$

where f takes on the values (t, b) and f_j stands for $\chi^{\pm}_j, \chi^0_j$ while $\tilde{q}_i$ can be $\tilde{b}_i, \tilde{t}_i$. The decay width $\Gamma(\tilde{q}_i \to f_j f)$ is given by

$$\begin{aligned}\Gamma(\tilde{q}_i \to f_j f) = {} & \frac{1}{4\pi m_i^3}[(m_j^2 + m_f^2 - m_i^2)^2 - 4m_j^2 m_f^2]^{1/2} \\ & \times \Big\{\frac{1}{2}(|B^S_{ij}|^2 + |B^P_{ij}|^2)(m_i^2 - m_j^2 - m_f^2) \\ & - \frac{1}{2}(|B^S_{ij}|^2 - |B^P_{ij}|^2) 2 m_j m_f \Big\}. \end{aligned} \tag{113}$$

The coefficients B^S_{ij} and B^P_{ij} contain the loop corrections and depend on the CP phases. Thus, for example, the process $\tilde{b}_i \to \chi^-_j + t$ gives the coefficients

$$\begin{aligned} B^S_{ij} &= \frac{g}{2}[R_{bij} + L_{bij} + \Delta R_{bij} + \Delta L_{bij}] \\ B^P_{ij} &= \frac{g}{2}[R_{bij} - L_{bij} + \Delta R_{bij} - \Delta L_{bij}] \end{aligned} \tag{114}$$

where R_{bij}, L_{bij}, ΔL_{bij} and ΔR_{bij} are defined by Eqs. (2), (43), and (44).

V. NUMERICAL ANALYSIS AND SIZE OF EFFECTS

In this section we discuss in a quantitative fashion the size of loop effects on the decay widths of the squarks into chargino and neutralinos. The analysis of Secs. II, III, and IV is quite general and valid for the minimal supersymmetric standard model. For the sake of numerical analysis we will limit the parameter space by working within the framework of the SUGRA models [24]. Specifically within the framework of the extended mSUGRA model including CP phases, we take as our parameter space at the grand unification scale to be the following: the universal scalar mass m_0, the universal gaugino mass $m_{1/2}$, the universal trilinear coupling $|A_0|$, the ratio of the Higgs vacuum expectation values $\tan\beta = \langle H_2\rangle/\langle H_1\rangle$ where H_2 gives mass to the up quarks and H_1 gives mass to the down quarks and the leptons. In addition, we take for CP phases the following: the phase θ_μ of the Higgs mixing parameter μ so that $\mu = |\mu| e^{i\theta_\mu}$, the phase α_{A_0} of the trilinear coupling where[1] $A_0 = |A_0| e^{i\alpha_{A_0}}$, and the phases ξ_i $(i = 1, 2, 3)$ of the $SU(3)_C$, $SU(2)_L$ and $U(1)_Y$ gauginos, so that $\tilde{m}_i = |\tilde{m}_i| e^{i\xi_i}$ $(i = 1, 2, 3)$ where m_i $(i = 1, 2, 3)$ are the $SU(3)_C$, $SU(2)_L$ and $U(1)_Y$ gaugino masses. We note that not all the phases are independent and only certain combinations of them appear in the analysis [8]. In the numerical analysis we compute the loop corrections and also analyze their dependence on the phases. The masses of particles involved in the analysis are ordered as follows: for squarks $m_{\tilde{q}_1} > m_{\tilde{q}_2}$, for charginos $m_{\chi^-_1} < m_{\chi^-_2}$, for neutralinos $m_{\chi^0_1} < m_{\chi^0_2} < m_{\chi^0_3} < m_{\chi^0_4}$, and for neutral Higgs $(m_{H1}, m_{H2}, m_{H3}) \to (m_H, m_h, m_A)$ in the limit of no CP mixing where m_H is the heavy CP even Higgs, m_h is the light CP even Higgs, and m_A is the CP odd Higgs.

In Fig. 5(a) we give a plot of the decay width of the heavy stop $(\tilde{t}_1)$ into light and heavy chargino, χ^+_1 and χ^+_2, i.e., a plot of $\Gamma(\tilde{t}_1 \to b\chi^+_{1,2})$ as a function of α_{A_0}. The plots

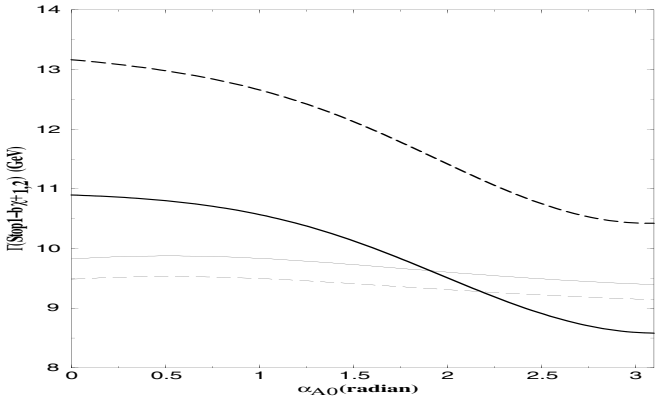

(a)

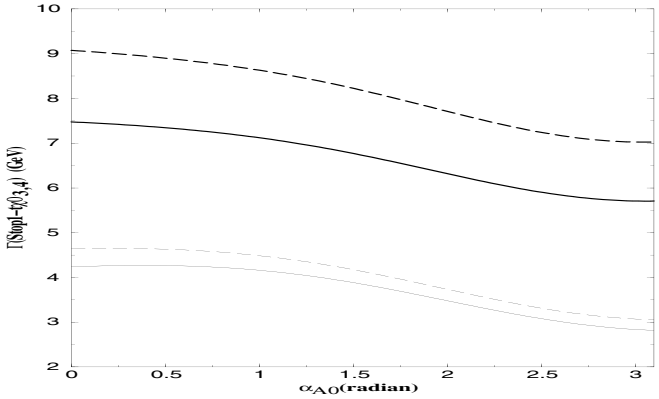

(b)

FIG. 5. (a) Plot of the decay width $\Gamma(\tilde{t}_1 \to b\chi^+_{1,2})$ as a function of α_{A_0}. The solid lines correspond to analysis at the tree level while the long-dashed lines include loop corrections. The input is $\tan\beta = 40$, $m_0 = 300$ GeV, $m_{1/2} = 300$ GeV, $\xi_1 = 0.5$ (radian), $\xi_2 = 0.66$ (radian), $\xi_3 = 0.63$ (radian), $\theta_\mu = 2.5$ (radian), and $|A_0| = 1$. The thick lines are for χ^+_2 decay and the thin lines are for χ^+_1 decay. (b) Plot of the decay width $\Gamma(\tilde{t}_1 \to t\chi^+_{3,4})$ as a function of α_{A_0}. The solid lines correspond to analysis at the tree level while the long-dashed lines include loop corrections. The input is $\tan\beta = 40$, $m_0 = 300$ GeV, $m_{1/2} = 300$ GeV, $\xi_1 = 0.5$ (radian), $\xi_2 = 0.66$ (radian), $\xi_3 = 0.63$ (radian), $\theta_\mu = 2.5$ (radian), and $|A_0| = 1$. The thick lines are for χ^0_4 decay and the thin lines are for χ^0_3 decay.

[1] A_0 enters in the off diagonal term in the squark mass^2 matrix in the form $m_q A^*_q m_0$ and is dimensionless.

are given with the analysis done at the tree level and at the level of the effective Lagrangian including loop corrections. The analysis shows that the loop effects can produce a correction of as much as 22% to the tree level values. Further, the analysis of Fig. 5(a) shows that the dependence on α_{A_0} is quite significant and both the tree and the loop corrections are affected by it. From Fig. 5(a) one finds that the variation with α_{A_0} in the range $(0, \pi)$ can be as much as 25%–30%. In Fig. 5(b) a similar plot is given for the decay width $\Gamma(\tilde{t}_1 \to t\chi^0_{3,4})$ as a function of α_{A_0}. Here one finds that the loop corrections can be as much as 20% and further that the variations with α_{A_0} can be as much as 25%–30%. However, loop correction itself does not have a strong dependence of α_{A_0} for this channel which leads to the difference between the tree level and the loop level being almost constant for the entire range. The effect of α_{A_0} on the decay width arises from two sources: (i) α_{A_0} enters the off diagonal elements of the squark mass[2] matrix. So it affects the squark masses that enter in the decay width. In fact, the modification of the squark masses due to α_{A_0} can be large enough that a decay channel may close or open as α_{A_0} is varied. This phenomenon will be illustrated explicitly later. This type of effect appears both at the tree and at the loop level. (ii) The matrix D_q that diagonalizes the squark matrix is sensitive to variations of α_{A_0} and this variation again affects both the tree and the loop level analysis. Thus at the tree level the couplings R_{qij}, L_{qij}, K_{qij} and M_{qij} depend on α_{A_0} and similarly at the loop level the couplings ΔR_{qij}, ΔL_{qij}, ΔK_{qij} and ΔM_{qij} also depend on α_{A_0}. An important phenomena related to the dependence on α_{A_0} is that the effects are strongly dependent on the quark mass. This is so because phases enter in the squark mass[2] matrix via the off diagonal terms in a prominent way and these off diagonal terms are proportional to the quark mass. Because of this, the sensitivity of the stop decay widths to α_{A_0} is far greater than the sensitivity of the sbottom decay width. The loop corrections are bigger in the case of the stop decay than for the sbottom case due to the relative difference of their Yukawa couplings. For this reason in our numerical analysis we will focus mostly on the effects of phases on stop decays.[2]

Figure 6(a) is a repeat of Fig. 5(a) with a plot of the light stop ($\tilde{t}_2$) decay width into charginos, i.e., $\Gamma(\tilde{t}_2 \to b\chi^+_{1,2})$ as a function of α_{A_0}. Here one finds that, while the loop corrections are comparable to the case of Fig. 5(a), the variations of the decay width is more strongly dependent on α_{A_0} in this part of the parameter space. Figure 6(b) gives an analysis similar to that of Fig. 5(b) where plots are given for the decay width $\Gamma(\tilde{t}_2 \to t\chi^0_{3,4})$ as a function of α_{A_0}. Here one finds that the loop corrections can be as much as 25%. Further, one finds that the variations with α_{A_0} are now much stronger than in the case of Fig. 5(b). Thus the effect of α_{A_0} is large enough that for values of $\alpha_{A_0} \geq 1.3$ (radian) the decays into χ^0_3, χ^0_4 are closed. The reason for this is purely kinematical, in that the mass of $\tilde{t}_2$ is strongly dependent on α_{A_0} and varies strongly with α_{A_0} and falls below the kinematical limit to allow for the decay into

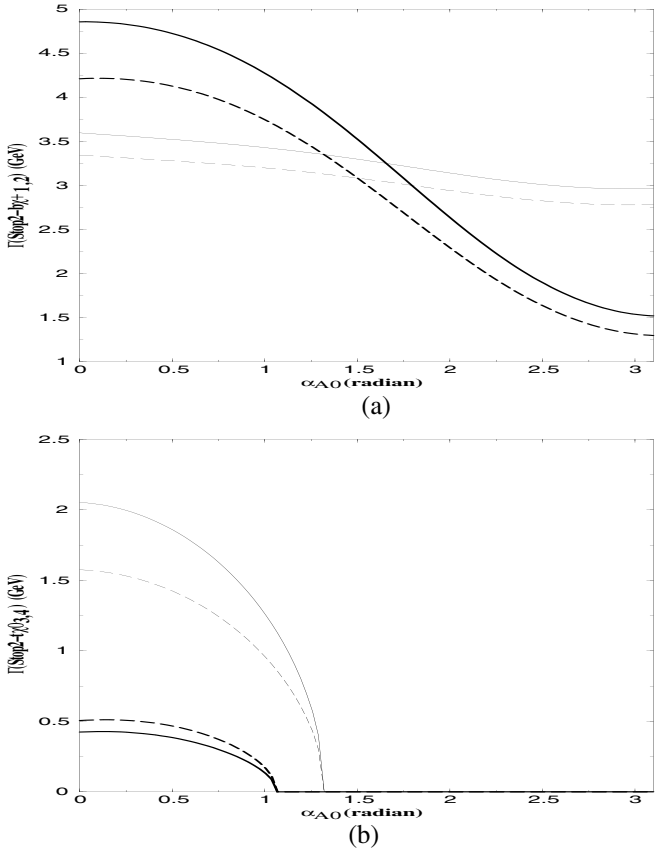

FIG. 6. (a) Plot of the decay width $\Gamma(\tilde{t}_2 \to b\chi^+_{1,2})$ as a function of α_{A_0}. The solid lines correspond to analysis at the tree level while the long-dashed lines include loop corrections. The input is $\tan\beta = 40$, $m_0 = 300$ GeV, $m_{1/2} = 300$ GeV, $\xi_1 = 0.5$ (radian), $\xi_2 = 0.66$ (radian), $\xi_3 = 0.63$ (radian), $\theta_\mu = 2.5$ (radian), and $|A_0| = 1$. The thick lines are for χ^+_2 decay and the thin lines are for χ^+_1 decay. (b) Plot of the decay width $\Gamma(\tilde{t}_2 \to t\chi^+_{3,4})$ as a function of α_{A_0}. The solid lines correspond to analysis at the tree level while the long-dashed lines include loop corrections. The input is $\tan\beta = 40$, $m_0 = 300$ GeV, $m_{1/2} = 300$ GeV, $\xi_1 = 0.5$ (radian), $\xi_2 = 0.66$ (radian), $\xi_3 = 0.63$ (radian), $\theta_\mu = 2.5$ (radian), and $|A_0| = 1$. The thick lines are for χ^0_4 decay and the thin lines are for χ^0_3 decay.

[2]A preliminary investigation of the effect of the SUSY QCD phase ξ_3 was given in Ref. [25] while in the present analysis we study the full set of loops and dependence on several phases both in the QCD and in the electroweak sector. The numerical analysis shows that the QCD and the electroweak contributions are typically comparable. Further, the QCD and the electroweak contributions can have similar or opposite signs depending on the part of the parameter space one is in. Thus contributions can either enhance or cancel each other allowing for a significant variation in the total contribution. In the region of large tanbeta the electroweak contribution arises mostly from Yukawa couplings.

χ_3^0, χ_4^0 for values of $\alpha_{A_0} \geq 1.3$. In Fig. 7(a) a plot is given of the decay width $\Gamma(\tilde{t}_1 \to b\chi^+, t\chi^0)$ (where we summed over the final states of charginos and neutralinos) both at the tree level and at the loop level as a function of α_{A_0}.

The analysis of Fig. 7(b) is similar to that of Fig. 7(a) except that one is looking at the decay width of $\tilde{t}_2$. The discontinuities in Fig. 7(b) are kinematical and arise from the closing of some of the neutralino final states. The analysis of Fig. 8(a) is similar to that of Fig. 7(a) while the analysis of Fig. 8(b) is similar to that of Fig. 7(b) except that the plots are made as a function of θ_μ. It is interesting to observe that the dependence of the stop widths on θ_μ in Fig. 8(b) appears to be relatively weaker. This arises because we are summing over the chargino and neutralino final states. Thus, for example, the decay width $\Gamma(\tilde{t}_1 \to b\chi_1^+)$ increases with θ_μ for the parameters of Fig. 8(a) while $\Gamma(\tilde{t}_1 \to b\chi_2^+)$ decreases. This results in the sum $\Gamma(\tilde{t}_1 \to b\chi_1^0, b\chi_2^+)$ having only a weak dependence on θ_μ. An analysis similar to that of Figs. 7(a) and 7(b) but as a function of ξ_3 is carried out in Figs. 9(a) and 9(b). One important new feature of the decay widths here is that the ξ_3 dependence of the widths at the tree level is absent while the loop corrected widths show a dependence on ξ_3. Here one finds that the loop corrections are typically of size 10%

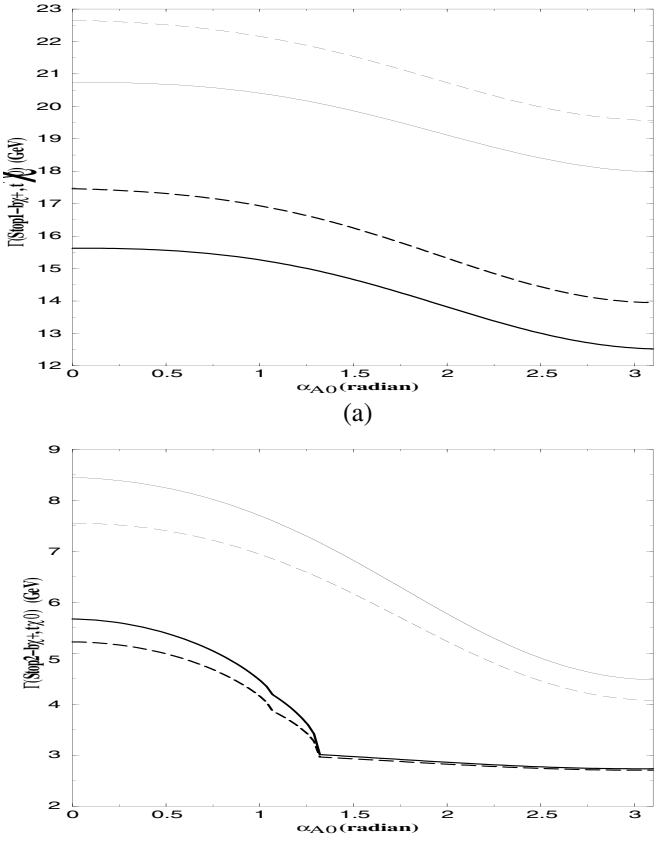

FIG. 7. (a) Plot of the decay width $\Gamma(\tilde{t}_1 \to b\chi^+, t\chi^0)$ as a function of α_{A_0}. The solid lines correspond to analysis at the tree level while the long-dashed lines include loop corrections. The input is $\tan\beta = 40$, $m_0 = 300$ GeV, $m_{1/2} = 300$ GeV, $\xi_1 = 0.5$ (radian), $\xi_2 = 0.66$ (radian), $\xi_3 = 0.63$ (radian), $\theta_\mu = 2.5$ (radian), and $|A_0| = 1$. The thick lines are for the sum over the neutralino final states and the thin lines are for the sum over the chargino final states. (b) Plot of the decay width $\Gamma(\tilde{t}_2 \to b\chi^+, t\chi^0)$ as a function of α_{A_0}. The solid lines correspond to analysis at the tree level while the long-dashed lines include loop corrections. The input is $\tan\beta = 40$, $m_0 = 300$ GeV, $m_{1/2} = 300$ GeV, $\xi_1 = 0.5$ (radian), $\xi_2 = 0.66$ (radian), $\xi_3 = 0.63$ (radian), $\theta_\mu = 2.5$ (radian), and $|A_0| = 1$. The thick lines are for the sum over the neutralino final states and the thin lines are for the sum over the chargino final states.

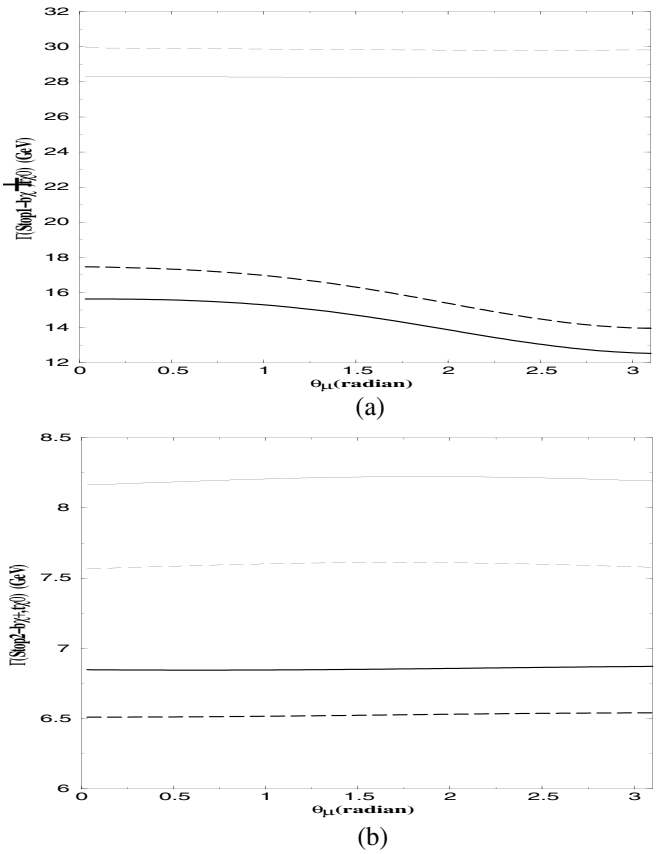

FIG. 8. (a) Plot of the decay width $\Gamma(\tilde{t}_1 \to b\chi^+, t\chi^0)$ as a function of θ_μ. The solid lines correspond to analysis at the tree level while the long-dashed lines include loop corrections. The input is $\tan\beta = 45$, $m_0 = 400$ GeV, $m_{1/2} = 400$ GeV, $\xi_1 = 0.6$ (radian), $\xi_2 = 0.65$ (radian), $\xi_3 = 0.65$ (radian), $\alpha_{A_0} = 2$ (radian), and $|A_0| = 1$. The thick lines are for the sum over the neutralino final states and the thin lines are for the sum over the chargino final states. (b) Plot of the decay width $\Gamma(\tilde{t}_2 \to b\chi^+, t\chi^0)$ as a function of θ_μ. The solid lines correspond to analysis at the tree level while the long-dashed lines include loop corrections. The input is $\tan\beta = 45$, $m_0 = 400$ GeV, $m_{1/2} = 400$ GeV, $\xi_1 = 0.6$ (radian), $\xi_2 = 0.65$ (radian), $\xi_3 = 0.65$ (radian), $\alpha_{A_0} = 2$ (radian), and $|A_0| = 1$. The thick lines are for the sum over the neutralino final states and the thin lines are for the sum over the chargino final states.

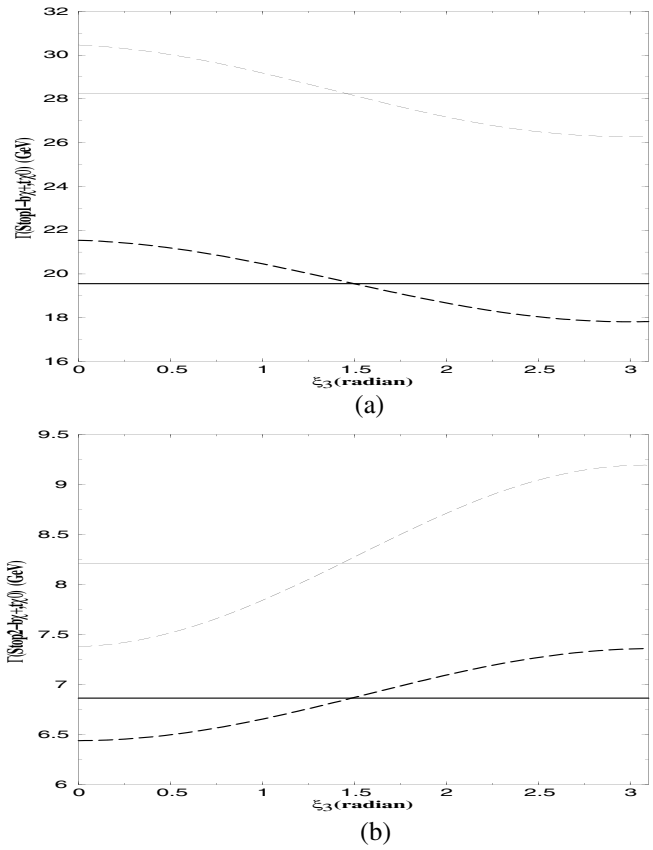

FIG. 9. (a) Plot of the decay width $\Gamma(\tilde{t}_1 \to b\chi^+, t\chi^0)$ as a function of ξ_3. The solid lines correspond to analysis at the tree level while the long-dashed lines include loop corrections. The input is $\tan\beta = 45$, $m_0 = 400$ GeV, $m_{1/2} = 400$ GeV, $\xi_1 = 0.6$ (radian), $\xi_2 = 0.65$ (radian), $\theta_\mu = 2.5$ (radian), $\alpha_{A_0} = 2$ (radian), and $|A_0| = 1$. The thick lines are for the sum over the neutralino final states and the thin lines are for the sum over the chargino final states. (b) Plot of the decay width $\Gamma(\tilde{t}_2 \to b\chi^+, t\chi^0)$ as a function of ξ_3. The solid lines correspond to analysis at the tree level while the long-dashed lines include loop corrections. The input is $\tan\beta = 45$, $m_0 = 400$ GeV, $m_{1/2} = 400$ GeV, $\xi_1 = 0.6$ (radian), $\xi_2 = 0.65$ (radian), $\theta_\mu = 2.5$ (radian), $\alpha_{A_0} = 2$ (radian), and $|A_0| = 1$. The thick lines are for the sum over the neutralino final states and the thin lines are for the sum over the chargino final states.

while the overall variation with ξ_3 can be as large as 15%. The loop correction to the sbottom decay is exhibited in Fig. 10 where the decay width $\Gamma(\tilde{b}_1 \to t\chi_1^-)$ is plotted. In this region of the parameter space the loop corrections to the sbottom decay are small and the dependence on α_{A_0} is also relatively small. The reasons for this weak dependence on the phase and the smallness of loop corrections have already been explained on an analytical basis at the end of the second paragraph of this section. Here we see that the reasoning presented there is borne out by the numerical analysis. Thus the largest loop corrections as well as the largest variations with phases arise only for the decay of the stops.

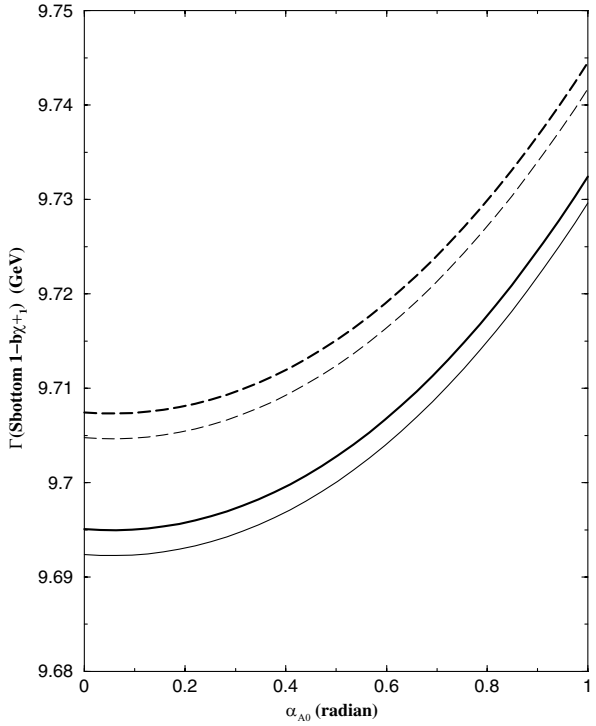

FIG. 10. Plot of the decay width $\Gamma(\tilde{b}_1 \to t\chi_1^-)$ as a function of α_{A_0}. The solid lines correspond to analysis at the tree level while the long-dashed lines include loop corrections. The input is $\tan\beta = 45$, $m_0 = 400$ GeV, $m_{1/2} = 400$ GeV, $\xi_1 = 0.6$ (radian), $\xi_2 = 0.65$ (radian), $\xi_3 = 0.65$ (radian), $\theta_\mu = 2.5$ (radian), and $|A_0| = 1$. The input for the thick lines is the same as for the thin lines except that $\xi_2 = 0.5$ (radian).

The experimental upper limits of the electric dipole moments are [11–13]: $|d_e| < 4.3 \times 10^{-27}$ e cm, $|d_n| < 6.5 \times 10^{-26}$ e cm and $|d_{Hg}| < 9.0 \times 10^{-28}$ e cm. The last constraint for Hg^{199} could be transformed into a constraint on a specific combination of the chromoelectric dipole moments of u, d and s quarks [9], $C_{Hg} = |d_d^C - d_u^C - 0.012 d_s^C| < 3.0 \times 10^{-26}$ cm. These constraints are satisfied by the cancellation mechanism in the numerical analysis presented above as follows: In Figs. 5–7, the constraints are satisfied for the inputs $\tan\beta = 40$, $m_0 = 300$ GeV, $m_{1/2} = 300$ GeV, $\xi_1 = 0.5$ (radian), $\xi_2 = 0.66$ (radian), $\xi_3 = 0.63$ (radian), $\theta_\mu = 2.5$ (radian), $\alpha_{A_0} = 1.0$ (radian) and $|A_0| = 1$. At this point we have $|d_e| = 1.88 \times 10^{-27}$ e cm, $|d_n| = 1.79 \times 10^{-27}$ e cm and $C_{Hg} = 8.99 \times 10^{-27}$ cm. In Figs. 8–10 they are satisfied for the inputs $\tan\beta = 45$, $m_0 = 400$ GeV, $m_{1/2} = 400$ GeV, $\xi_1 = 0.6$ (radian), $\xi_2 = 0.65$ (radian), $\xi_3 = 0.65$ (radian), $\theta_\mu = 2.5$ (radian), $\alpha_{A_0} = 2.0$ (radian) and $|A_0| = 1$. At this point we have $|d_e| = 3.94 \times 10^{-27}$ e cm, $|d_n| = 9.21 \times 10^{-27}$ e cm and $C_{\rm Hg} = 3.86 \times 10^{-27}$ cm.

As pointed out in the beginning of this section, the parameter space of the model is quite large, consisting of m_0, $m_{1/2}$, $|A_0|$, $\tan\beta$, θ_μ, α_A, and ξ_i. Thus there are many possibilities for studying numerically the sensitivity of the

loop contributions with respect to these parameters. In the numerical analysis presented above we studied the sensitivity of the loop corrections with respect to α_A, θ_μ and ξ_3. We give now an analysis of the sensitivity of the loop contributions with respect to $\tan\beta$ and with respect to ξ_2. In Fig. 11 we give a plot of the decay widths $\Gamma(\tilde{t}_1 \to b\chi_i^+)$, $\Gamma(\tilde{t}_2 \to b\chi_i^+)$, and $\Gamma(\tilde{t}_1 \to t\chi_j^0)$, and $\Gamma(\tilde{t}_2 \to t\chi_j^0)$ as a function of $\tan\beta$. The loop corrections could be as 30% or even larger. One finds that the decays into charginos are typically more sensitive to $\tan\beta$ than decays into neutralinos and the loop contribution shows the same sensitivity. In part, this arises because the chargino mass matrix and the neutralino mass matrix have different dependence on $\tan\beta$. The kink in the decay width of the stop one into neutralinos is just a kinematical threshold effect. In Fig. 12 we give a plot of the decay widths $\Gamma(\tilde{t}_1 \to b\chi_i^+)$, $\Gamma(\tilde{t}_2 \to b\chi_i^+)$, and $\Gamma(\tilde{t}_1 \to t\chi_j^0)$, and $\Gamma(\tilde{t}_2 \to t\chi_j^0)$ as a function of ξ_2. Here one finds that both the tree as well as the loop contribution have a fairly significant dependence on ξ_2 and the loop corrections are in general non-negligible with the largest effect occurring for the decay of stop one into charginos. In this case the value of the edms at $\xi_2 = 1.2$ radian are $|d_e| = 1.1 \times 10^{-27}$ e cm, $|d_n| = 2.9 \times 10^{-26}$ e cm, $C_{\rm Hg} = 1.2 \times 10^{-26}$ cm all within the current experimental bounds.

We give now a brief comparison with some of the previous works. The analysis of Ref. [2] is at the tree level and our analysis is in agreement with it ignoring loops. With inclusion of loops the pertinent works are Refs. [3–6]. In the work of Ref. [3] only two diagrams of the present analysis are calculated, and they correspond to the vertex corrections from Figs. 1(b) and 1(c) of our analysis. Further, their analysis is done in the Yukawa approximation. Specifically, for Fig. 1(b) this approximation can be gotten from our Eqs. (9) and (10) by retaining only the terms that contain α_{bl} and α_{tl} in the expressions for $\Delta R^{(2)}_{bij}$ and $\Delta L^{(2)}_{bij}$. Similarly, in the analysis of Fig. 1(c) the

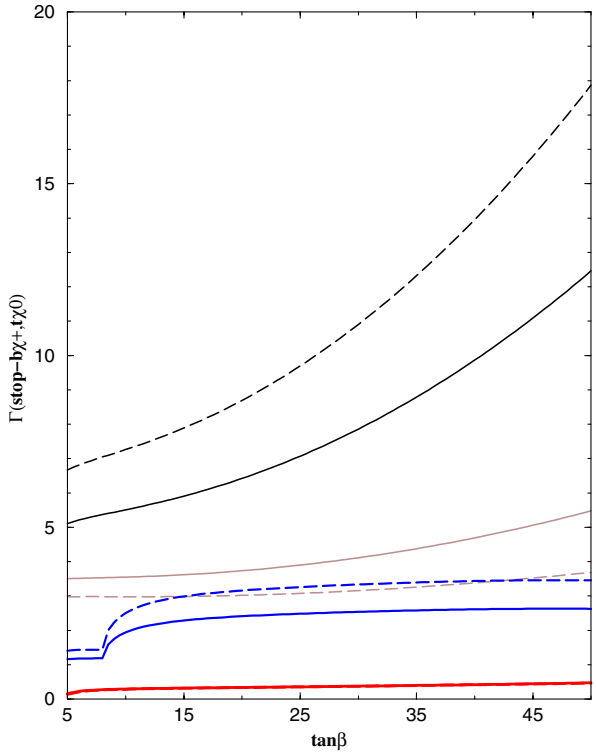

FIG. 11 (color online). Plot of the decay width $\Gamma(\tilde{t}_{1,2} \to b\chi_i^+)$ and $\Gamma(\tilde{t}_{1,2} \to t\chi_j^0)$ as a function of $\tan\beta$. The solid lines correspond to analysis at the tree level while the long-dashed lines include loop corrections. The input is $m_0 = 100$ GeV, $m_1/2 = 120$ GeV, $A_0 = 0$ and all phases are set to zero. The curves in descending order at $\tan\beta = 5$ correspond to decay widths for $\Gamma(\tilde{t}_1 \to b\chi_i^+)$, $\Gamma(\tilde{t}_2 \to b\chi_i^+)$, $\Gamma(\tilde{t}_1 \to t\chi_j^0)$, and $\Gamma(\tilde{t}_2 \to t\chi_j^0)$. In each case all kinematically allowed chargino or neutralino final states in the decay are included in the analysis. The tree calculation and the loop calculation coincide for the bottommost curve.

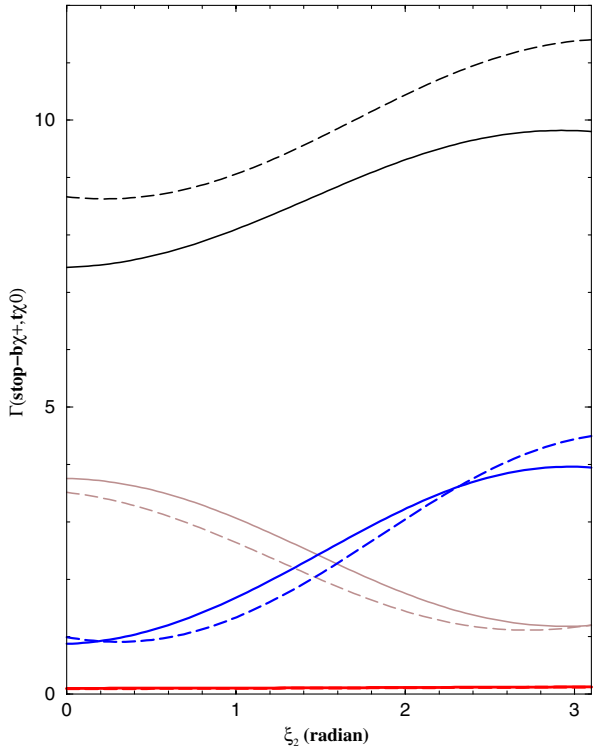

FIG. 12 (color online). Plot of the decay width $\Gamma(\tilde{t}_{1,2} \to b\chi_i^+)$ and $\Gamma(\tilde{t}_{1,2} \to t\chi_j^0)$ as a function of ξ_2. The solid lines correspond to analysis at the tree level while the long-dashed lines include loop corrections. The input is $\tan\beta = 30$, $m_0 = 110$ GeV, $m_1/2 = 105$ GeV, $\xi_1 = 0.43$, $\xi_3 = 1.12$, $\theta_\mu = 2$, $\alpha_{A0} = 1$, and $|A_0| = 1$ The edms constraints are satisfied at $\xi_2 = 1.2$ The curves in descending order at $\xi_2 = 0$ correspond to decay widths for $\Gamma(\tilde{t}_1 \to b\chi_i^+)$, $\Gamma(\tilde{t}_2 \to b\chi_i^+)$, $\Gamma(\tilde{t}_1 \to t\chi_j^0)$, and $\Gamma(\tilde{t}_2 \to t\chi_j^0)$. In each case all kinematically allowed chargino or neutralino final states are included in the analysis. The tree calculation and the loop calculation coincide for the bottommost curve.

Yukawa approximation corresponds to retaining only the last terms in Eqs. (16) and (17). Within the above approximation and setting the phases to zero, our analysis is in agreement with their Figs. 3–5 for their inputs. In Ref. [6] the authors study the one loop correction from the SUSY electroweak sector but not from the QCD sector. There are no analytic results as the analysis is done on a computer. Ignoring the QCD correction, and setting the phases to zero, our analysis is in numerical agreement with theirs Figs. 1–3. In Ref. [4] the authors calculate only the QCD correction and do not take into account the SUSY electroweak correction. Within that approximation and setting the phases to zero, our part of the analysis which produces QCD effects is in agreement with their Figs. 2–5 for their inputs. The work of Ref. [5] takes into account the *CP* phases but only three diagrams corresponding to our diagrams 2(b), 2(d), and 2(e) are computed and thus this analysis is also partial.

VI. CONCLUSION

In this paper we have analyzed supersymmetric one loop corrections to the squark-quark-chargino and to the squark-quark-neutralino couplings. The analysis involves the exchange of the gluino, chargino, neutralino, W, Z, charged Higgs and neutral Higgs. With the above analysis the one loop effective Lagrangian for these interactions was derived. The full *CP* dependence arising from the soft *CP* parameters was taken into account in the analysis. The effective Lagrangian was then used to obtain the decay of the squarks into charginos and neutralinos at the one loop order. A detailed numerical analysis within extended SUGRA model was then carried out to study the size of the loop effects and also to study the effect of *CP* phases on the decay widths of the squarks into charginos and neutralinos. The analysis exhibits that the loop corrections to the decays widths of the stops can be very substantial, i.e., as much as 30% or more. Further, the phase dependence of the decay width is found to be very strong producing a variation of as much as 25%–30% or more. The phases enter in the decay widths in two ways; in modifying the stop-bottom-chargino, and the stop-top-neutralino couplings and in modifying the stop, chargino and neutralino masses. In some cases the effect of phases is large enough to open or close a decay channel. However, a similar analysis for the decay of the sbottoms shows the effect of loops as well as the effect of *CP* phases to be much smaller. The one loop effective Lagrangian derived in this paper would be useful in the analysis of squark decays at colliders and in connecting experimental data with the underlying theoretical schemes such as supergravity and string based models.

ACKNOWLEDGMENTS

This research was supported in part by NSF Grant No. PHY-0139967.

APPENDIX

For completeness we give below the loop corrections to the Yukawa couplings Δh_b, δh_b etc. that appear in Sec. II. A derivation of these results can be found in [16,18].

$$
\begin{aligned}
-\Delta h_b = &-\sum_{i=1}^{2}\sum_{j=1}^{2}\frac{2\alpha_s}{3\pi}e^{-i\xi_3}m_{\tilde{g}}G^*_{ij}D^*_{b1i}D_{b2j}f(m^2_{\tilde{g}},m^2_{\tilde{b}_i},m^2_{\tilde{b}_j})-\sum_{i=1}^{2}\sum_{j=1}^{2}\sum_{k=1}^{2}g^2E^*_{ij}\{V^*_{k1}D^*_{t1i}-K_tV^*_{k2}D^*_{t2i}\}\\
&\times(K_bU^*_{k2}D_{t1j})\frac{m_{\chi^+_k}}{16\pi^2}f(m^2_{\chi^+_k},m^2_{\tilde{t}_i},m^2_{\tilde{t}_j})-\sum_{i=1}^{2}\sum_{j=1}^{2}\sum_{k=1}^{2}g^2C_{ij}\{V^*_{i1}D^*_{t1k}-K_tV^*_{i2}D^*_{t2k}\}(K_bU^*_{j2}D_{t1k})\\
&\times\frac{m_{\chi^+_i}m_{\chi^+_j}}{16\pi^2}f(m^2_{\tilde{t}_k},m^2_{\chi^+_i},m^2_{\chi^+_j})+\sum_{i=1}^{2}\sum_{j=1}^{2}\sum_{k=1}^{4}2G^*_{ij}\{\alpha_{bk}D_{b1j}-\gamma_{bk}D_{b2j}\}\{\beta^*_{bk}D^*_{b1i}+\alpha_{bk}D^*_{b2i}\}\frac{m_{\chi^0_k}}{16\pi^2}f(m^2_{\chi^0_k},m^2_{\tilde{b}_i},m^2_{\tilde{b}_j})\\
&+\sum_{i=1}^{4}\sum_{j=1}^{4}\sum_{k=1}^{2}2\Gamma_{ij}\{\alpha_{bj}D_{b1k}-\gamma_{bj}D_{b2k}\}\{\beta^*_{bi}D^*_{b1k}+\alpha_{bi}D^*_{b2k}\}\frac{m_{\chi^0_i}m_{\chi^0_j}}{16\pi^2}f(m^2_{\tilde{b}_k},m^2_{\chi^0_i},m^2_{\chi^0_j})
\end{aligned}
\tag{A1}
$$

$$
\frac{C_{ij}}{\sqrt{2}}=-\frac{g}{\sin\beta}\left[\frac{m_{\chi^+_i}}{2M_W}\delta_{ij}-Q^*_{ij}\cos\beta-R^*_{ij}\right]
\tag{A2}
$$

$$
\frac{\Gamma_{ij}}{\sqrt{2}}=-\frac{g}{2\sin\beta}\left[\frac{m_{\chi^0_i}}{2M_W}\delta_{ij}-Q''^*_{ij}\cos\beta-R''^*_{ij}\right]
\tag{A3}
$$

$$
\begin{aligned}
R_{ij}&=\frac{1}{2M_W}[\tilde{m}^*_2U_{i1}V_{j1}+\mu^*U_{i2}V_{j2}]\qquad gQ''_{ij}=\frac{1}{2}[X^*_{3i}(gX^*_{2j}-g'X^*_{1j})+(i\leftrightarrow j)]\\
R''_{ij}&=\frac{1}{2M_W}[\tilde{m}^*_1X^*_{1i}X^*_{1j}+\tilde{m}^*_2X^*_{2i}X^*_{2j}-\mu^*(X^*_{3i}X^*_{4j}+X^*_{4i}X^*_{3j})]
\end{aligned}
\tag{A4}
$$

$$-\delta h_b = -\sum_{i=1}^{2}\sum_{j=1}^{2}\frac{2\alpha_s}{3\pi}e^{-i\xi_3}m_{\tilde g}H_{ji}D^*_{b1i}D_{b2j}f(m^2_{\tilde g},m^2_{\tilde b_i},m^2_{\tilde b_j})-\sum_{i=1}^{2}\sum_{j=1}^{2}\sum_{k=1}^{2}g^2F_{ji}\{V^*_{k1}D^*_{t1i}-K_tV^*_{k2}D^*_{t2i}\}(K_bU^*_{k2}D_{t1j})$$
$$\times\frac{m_{\chi^+_k}}{16\pi^2}f(m^2_{\chi^+_k},m^2_{\tilde t_i},m^2_{\tilde t_j})+\sum_{i=1}^{2}\sum_{j=1}^{2}\sum_{k=1}^{4}2H_{ji}\{\alpha_{bk}D_{b1j}-\gamma_{bk}D_{b2j}\}\{\beta^*_{bk}D^*_{b1i}+\alpha_{bk}D^*_{b2i}\}\frac{m_{\chi^0_k}}{16\pi^2}f(m^2_{\chi^0_k},m^2_{\tilde b_i},m^2_{\tilde b_j}) \tag{A5}$$

$$-\Delta h_t = -\sum_{i=1}^{2}\sum_{j=1}^{2}\frac{2\alpha_s}{3\pi}e^{-i\xi_3}m_{\tilde g}F^*_{ij}D^*_{t1i}D_{t2j}f(m^2_{\tilde g},m^2_{\tilde t_i},m^2_{\tilde t_j})-\sum_{i=1}^{2}\sum_{j=1}^{2}\sum_{k=1}^{2}g^2H^*_{ij}\{U^*_{k1}D^*_{b1i}-K_bU^*_{k2}D^*_{b2i}\}(K_tV^*_{k2}D_{b1j})$$
$$\times\frac{m_{\chi^+_k}}{16\pi^2}f(m^2_{\chi^+_k},m^2_{\tilde b_i},m^2_{\tilde b_j})-\sum_{i=1}^{2}\sum_{j=1}^{2}\sum_{k=1}^{2}g^2K^*_{ij}\{U^*_{i1}D^*_{b1k}-K_bU^*_{i2}D^*_{b2k}\}(K_tV^*_{j2}D_{b1k})\frac{m_{\chi^+_i}m_{\chi^+_j}}{16\pi^2}f(m^2_{\tilde b_k},m^2_{\chi^+_i},m^2_{\chi^+_j})$$
$$+\sum_{i=1}^{2}\sum_{j=1}^{2}\sum_{k=1}^{4}2F^*_{ij}\{\alpha_{tk}D_{t1j}-\gamma_{tk}D_{t2j}\}\{\beta^*_{tk}D^*_{t1i}+\alpha_{tk}D^*_{t2i}\}\frac{m_{\chi^0_k}}{16\pi^2}f(m^2_{\chi^0_k},m^2_{\tilde t_i},m^2_{\tilde t_j})$$
$$+\sum_{i=1}^{4}\sum_{j=1}^{4}\sum_{k=1}^{2}2\Delta^*_{ij}\{\alpha_{tj}D_{t1k}-\gamma_{tj}D_{t2k}\}\{\beta^*_{ti}D^*_{t1k}+\alpha_{ti}D^*_{t2k}\}\frac{m_{\chi^0_i}m_{\chi^0_j}}{16\pi^2}f(m^2_{\tilde t_k},m^2_{\chi^0_i},m^2_{\chi^0_j}) \tag{A6}$$

where

$$K_{ij}=-\sqrt{2}gQ_{ji} \tag{A7}$$

$$\Delta_{ij}=-\frac{g}{\sqrt{2}}Q''_{ij} \tag{A8}$$

$$-\delta h_t = -\sum_{i=1}^{2}\sum_{j=1}^{2}\frac{2\alpha_s}{3\pi}e^{-i\xi_3}m_{\tilde g}E_{ji}D^*_{t1i}D_{t2j}f(m^2_{\tilde g},m^2_{\tilde t_i},m^2_{\tilde t_j})-\sum_{i=1}^{2}\sum_{j=1}^{2}\sum_{k=1}^{2}g^2G_{ji}\{U^*_{k1}D^*_{b1i}-K_bU^*_{k2}D^*_{b2i}\}(K_tV^*_{k2}D_{b1j})$$
$$\times\frac{m_{\chi^+_k}}{16\pi^2}f(m^2_{\chi^+_k},m^2_{\tilde b_i},m^2_{\tilde b_j})+\sum_{i=1}^{2}\sum_{j=1}^{2}\sum_{k=1}^{4}2E_{ji}\{\alpha_{tk}D_{t1j}-\gamma_{tk}D_{t2j}\}\{\beta^*_{tk}D^*_{t1i}+\alpha_{tk}D^*_{t2i}\}\frac{m_{\chi^0_k}}{16\pi^2}f(m^2_{\chi^0_k},m^2_{\tilde t_i},m^2_{\tilde t_j}) \tag{A9}$$

$$-\overline{\Delta h}_b = -\sum_{i=1}^{2}\sum_{j=1}^{2}\frac{2\alpha_s}{3\pi}e^{-i\xi_3}D_{b2j}D^*_{t1i}\eta^*_{ji}m_{\tilde g}f(m^2_{\tilde g},m^2_{\tilde t_i},m^2_{\tilde b_j})+\sum_{i=1}^{2}\sum_{j=1}^{2}\sum_{k=1}^{4}2\eta^*_{ji}(\alpha_{bk}D_{b1j}-\gamma_{bk}D_{b2j})(\beta^*_{tk}D^*_{t1i}+\alpha_{tk}D^*_{t2i})$$
$$\times\frac{m_{\chi^0_k}}{16\pi^2}f(m^2_{\chi^0_k},m^2_{\tilde t_i},m^2_{\tilde b_j})+\sum_{i=1}^{2}\sum_{j=1}^{2}\sum_{k=1}^{4}\sqrt{2}\,g\xi_{ki}\frac{m_{\chi^0_k}m_{\chi^-_i}}{16\pi^2}[-K_bU^*_{i2}D_{t1j}(\beta^*_{tk}D^*_{t1j}+\alpha_{tk}D^*_{t2j})f(m^2_{\tilde t_j},m^2_{\chi^-_i},m^2_{\chi^0_k})$$
$$+(\alpha_{bk}D_{b1j}-\gamma_{bk}D_{b2j})(U^*_{i1}D^*_{b1j}-K_bU^*_{i2}D^*_{b2j})f(m^2_{\tilde b_j},m^2_{\chi^-_i},m^2_{\chi^0_k})] \tag{A10}$$

$$-\overline{\delta h}_b = \sum_{i=1}^{2}\sum_{j=1}^{2}\frac{2\alpha_s}{3\pi}e^{-i\xi_3}D_{b2j}D^*_{t1i}\eta'_{ji}m_{\tilde g}f(m^2_{\tilde g},m^2_{\tilde t_i},m^2_{\tilde b_j})-\sum_{i=1}^{2}\sum_{j=1}^{2}\sum_{k=1}^{4}2\eta'_{ji}(\alpha_{bk}D_{b1j}-\gamma_{bk}D_{b2j})(\beta^*_{tk}D^*_{t1i}+\alpha_{tk}D^*_{t2i})$$
$$\times\frac{m_{\chi^0_k}}{16\pi^2}f(m^2_{\chi^0_k},m^2_{\tilde t_i},m^2_{\tilde b_j}) \tag{A11}$$

$$-\overline{\Delta h}_t = -\sum_{i=1}^{2}\sum_{j=1}^{2}\frac{2\alpha_s}{3\pi}e^{-i\xi_3}D^*_{b1i}D_{t2j}\eta'^*_{ij}m_{\tilde{g}}f(m^2_{\tilde{g}},m^2_{\tilde{b}_i},m^2_{\tilde{t}_j})+\sum_{i=1}^{2}\sum_{j=1}^{2}\sum_{k=1}^{4}2\eta'^*_{ij}(\alpha_{tk}D_{t1j}-\gamma_{tk}D_{t2j})(\beta^*_{bk}D^*_{b1i}+\alpha_{bk}D^*_{b2i})$$
$$\times\frac{m_{\chi^0_k}}{16\pi^2}f(m^2_{\chi^0_k},m^2_{\tilde{b}_i},m^2_{\tilde{t}_j})+\sum_{i=1}^{2}\sum_{j=1}^{2}\sum_{k=1}^{4}\sqrt{2}\,g\xi'^*_{ki}\frac{m_{\chi^0_k}m_{\chi^-_i}}{16\pi^2}[-K_tV^*_{i2}D_{b1j}(\beta^*_{bk}D^*_{b1j}+\alpha_{bk}D^*_{b2j})f(m^2_{\tilde{b}_j},m^2_{\chi^-_i},m^2_{\chi^0_k})$$
$$+(\alpha_{tk}D_{t1j}-\gamma_{tk}D_{t2j})(V^*_{i1}D^*_{t1j}-K_tV^*_{i2}D^*_{t2j})f(m^2_{\tilde{t}_j},m^2_{\chi^-_i},m^2_{\chi^0_k})] \tag{A12}$$

$$-\overline{\delta h}_t = \sum_{i=1}^{2}\sum_{j=1}^{2}\frac{2\alpha_s}{3\pi}e^{-i\xi_3}D^*_{b1i}D_{t2j}\eta_{ij}m_{\tilde{g}}f(m^2_{\tilde{g}},m^2_{\tilde{b}_i},m^2_{\tilde{t}_j})-\sum_{i=1}^{2}\sum_{j=1}^{2}\sum_{k=1}^{4}2\eta_{ij}(\alpha_{tk}D_{t1j}-\gamma_{tk}D_{t2j})(\beta^*_{bk}D^*_{b1i}+\alpha_{bk}D^*_{b2i})$$
$$\times\frac{m_{\chi^0_k}}{16\pi^2}f(m^2_{\chi^0_k},m^2_{\tilde{b}_i},m^2_{\tilde{t}_j}). \tag{A13}$$

[1] A. Bartl *et al.*, Phys. Lett. B **435**, 118 (1998); A. Bartl *et al.*, Phys. Lett. B **460**, 157 (1999); K. Hidaka and A. Bartl, Phys. Lett. B **501**, 78 (2001); C. Weber, H. Eberl, and W. Majerotto, Phys. Rev. D **68**, 093011 (2003); W. M. Yang and D. S. Du, Phys. Rev. D **65**, 115005 (2002).

[2] A. Bartl, S. Hesselbach, K. Hidaka, T. Kernreiter, and W. Porod, Phys. Rev. D **70**, 035003 (2004).

[3] J. Guasch *et al.*, Phys. Lett. B **437**, 88 (1998).

[4] S. Kraml *et al.*, Phys. Lett. B **386**, 175 (1996).

[5] M. Aoki and N. Oshimo, Mod. Phys. Lett. A **13**, 3225 (1998).

[6] J. Guasch *et al.*, Phys. Lett. B **510**, 211 (2001).

[7] P. Nath, Phys. Rev. Lett. **66**, 2565 (1991); Y. Kizukuri and N. Oshimo, Phys. Rev. D **46**, 3025 (1992).

[8] T. Ibrahim and P. Nath, Phys. Lett. B **418**, 98 (1998); Phys. Rev. D **57**, 478 (1998); **58**, 111301 (1998); T. Falk and K, Olive, Phys. Lett. B **439**, 71 (1998); M. Brhlik, G. J. Good, and G. L. Kane, Phys. Rev. D **59**, 115004 (1999); A. Bartl, E. Christova, T. Gojdosik, and W. Majerotto, Phys. Rev. D **59**, 077503 (1999); S. Pokorski, J. Rosiek, and C. A. Savoy, Nucl. Phys. B **570**, 81 (2000); E. Accomando, R. Arnowitt, and B. Dutta, Phys. Rev. D **61**, 115003 (2000); U. Chattopadhyay, T. Ibrahim, D. P. Roy, Phys. Rev. D **64**, 013004 (2001); C. S. Huang and W. Liao, Phys. Rev. D **61**, 116002 (2000); **62**, 016008 (2000); A. Bartl, T. Gajdosik, E. Lunghi, A. Masiero, W. Porod, H. Stremnitzer, and O. Vives, Phys. Rev. D **64**, 076009 (2001); M. Brhlik, L. Everett, G. Kane, and J. Lykken, Phys. Rev. Lett. **83**, 2124 (1999); Phys. Rev. D **62**, 035005 (2000); E. Accomando, R. Arnowitt, and B. Datta, Phys. Rev. D **61**, 075010 (2000); T. Ibrahim and P. Nath, Phys. Rev. D **61**, 093004 (2000).

[9] T. Falk, K. A. Olive, M. Prospelov, and R. Roiban, Nucl. Phys. B **560**, 3 (1999); V. D. Barger, T. Falk, T. Han, J. Jiang, T. Li, and T. Plehn, Phys. Rev. D **64**, 056007 (2001); S. Abel, S. Khalil, and O. Lebedev, Phys. Rev. Lett. **86**, 5850 (2001); T. Ibrahim and P. Nath, Phys. Rev. D **67**, 016005 (2003).

[10] D. Chang, W.-Y. Keung, and A. Pilaftsis, Phys. Rev. Lett. **82**, 900 (1999).

[11] E. Commins *et al.*, Phys. Rev. A **50**, 2960 (1994).

[12] P. G. Harris *et al.*, Phys. Rev. Lett. **82**, 904 (1999).

[13] S. K. Lamoreaux, J. P. Jacobs, B. R. Heckel, F. J. Raab, and E. N. Fortson, Phys. Rev. Lett. **57**, 3125 (1986).

[14] A. Pilaftsis, Phys. Rev. D **58**, 096010 (1998); Phys. Lett. B **435**, 88 (1998); A. Pilaftsis and C. E. M. Wagner, Nucl. Phys. B **553**, 3 (1999); D. A. Demir, Phys. Rev. D **60**, 055006 (1999); S. Y. Choi, M. Drees, and J. S. Lee, Phys. Lett. B **481**, 57 (2000); T. Ibrahim and P. Nath, Phys. Rev. D **63**, 035009 (2001); T. Ibrahim, Phys. Rev. D **64**, 035009 (2001); T. Ibrahim and P. Nath, Phys. Rev. D **66**, 015005 (2002); S. W. Ham, S. K. Oh, E. J. Yoo, C. M. Kim, and D. Son, Phys. Rev. D **68**, 055003 (2003); M. Boz, Mod. Phys. Lett. A **17**, 215 (2002); M. Carena, J. R. Ellis, A. Pilaftsis, and C. E. Wagner, Nucl. Phys. B **625**, 345 (2002); A. Dedes and A. Pilaftsis, Phys. Rev. D **67**, 015012 (2003); J. Ellis, J. S. Lee, and A. Pilaftsis, Phys. Rev. D **70**, 075010 (2004).

[15] E. Christova, H. Eberl, W. Majerotto, and S. Kraml, J. High Energy Phys. 12 (2002) 021; E. Christova, H. Eberl, W. Majerotto, and S. Kraml, Nucl. Phys. B **639**, 263 (2002); **647**, 359(E) (2002).

[16] T. Ibrahim and P. Nath, Phys. Rev. D **67**, 095003 (2003).

[17] T. Ibrahim and P. Nath, Phys. Rev. D **68**, 015008 (2003).

[18] T. Ibrahim and P. Nath, Phys. Rev. D **69**, 075001 (2004).

[19] T. Ibrahim, P. Nath, and A. Psinas, Phys. Rev. D **70**, 035006 (2004).

[20] U. Chattopadhyay, T. Ibrahim, and P. Nath, Phys. Rev. D **60**, 063505 (1999); T. Falk, A. Ferstl, and K. Olive, Astropart. Phys. **13**, 301 (2000); P. Gondolo and K. Freese, J. High Energy Phys. 07 (2002) 052.

[21] M. E. Gomez, T. Ibrahim, P. Nath, and S. Skadhauge, Phys. Rev. D **70**, 035014 (2004); hep-ph/0410007; T. Nihei and M. Sasagawa, Phys. Rev. D **70**, 055011 (2004); **70**, 079901 (2004).

[22] For a more complete set of references, see T. Ibrahim and P. Nath, hep-ph/0210251, published in P. Nath and P. M. Zerwas, Supersymmetry and Unification of Fundamental Interactions. Proceedings of the 10th International Conference, SUSY'02, Hamburg, Germany, 2002, DESY-PROC-2002-02.

[23] For a recent review, see M. Carena and H. E. Haber, Prog. Part. Nucl. Phys. **50**, 63 (2003).

[24] A. H. Chamseddine, R. Arnowitt, and P. Nath, Phys. Rev. Lett. **49**, 970 (1982); R. Barbieri, S. Ferrara, and C. A. Savoy, Phys. Lett. B **119**, 343 (1982); L. Hall, J. Lykken, and S. Weinberg, Phys. Rev. D **27**, 2359 (1983); P. Nath, R. Arnowitt, and A. H. Chamseddine, Nucl. Phys. B **227**, 121 (1983). For a recent review, see P. Nath, hep-ph/0307123.

[25] T. Ibrahim, in Proceedings of PASCOS04 Symposium, Boston, 2004.